FOREWORD

This work was conducted by the National Carbon Company, A Division of Union Carbide Corporation under USAF Contract AF 33(616)-6915. This contract was initiated under Project No. 7350 "Refractory Inorganic Non-Metallic Materials," Task No. 735002 "Graphite Materials Development;" Project No. 7381 "Materials Application," Task No. 738102 "Materials Preproduction Process Development;" and Project No. 7-817 "Process Development for Graphite Materials." The work was administrated under the direction of the Directorate of Materials and Processes, Deputy for Technology, Aeronautical Systems Division, with Captain R. H. Wilson, L. J. Conlon and W. P. Conrardy acting as Project Engineers.

The process for the production of the graphite described herein was developed by National Carbon Company prior to support from Contract AF 33(616)-6915. Initial scale-up efforts were supported by Contract LMSD 18-612 NOrd 17017. Subsequent scale-up and characterization of these materials were supported by Contract AF 33(616)-6915. This report covers work conducted from June 1957 through June 1961.

This is the seventh of a series of volumes of WADD Technical Report 61-72 prepared to describe various phases of work. The preceding volumes of this series are:

Volume I - Observations by Electron Microscopy of Dislocations in Graphite, by Richard Sprague.

Volume II - Applications of Anisotropic Elastic Continuum Theory to Dislocations in Graphite, by G. B. Spence.

Volume III - Decoration of Dislocations and Low Angle Grain Boundaries in Graphite Single Crystals, by Roger Bacon and Richard Sprague.

Volume IV - Adaptation of Radiographic Principles to the Quality Control of Graphite, by R. W. Wallouch.

Volume V - Analysis of Creep and Recovery Curves for ATJ Graphite, by E. J. Seldin and R. N. Draper.

Volume VI - Creep of Carbons and Graphites in Flexure at High Temperatures, by E. J. Seldin.

TABLE OF CONTENTS

LIST OF ILLUSTRATIONS

LIST OF ILLUSTRATIONS (CONT'D.)

FIGURE PAGE

LIST OF TABLES

LIST OF TABLES (CONT'D.)

1. INTRODUCTION

The manufacture of standard commercial graphite as generally practiced in industry differs greatly from that of metals since graphite has no distinct melting point at reasonable pressures, and the usual methods of forming such as casting, rolling, or other metalworking techniques cannot be employed. The graphite used in industry is manufactured from carbon base material, rather than mined as the natural substance. For this reason it is frequently called "artificial graphite". The graphite industry uses a process akin to that of the ceramic, but differing sharply in that a thermoplastic binder is used.

Graphite can be manufactured from almost any organic material that leaves a high carbon residue when heated. Petroleum coke, a refinery by-product, is, by far, the major source of graphite today. In manufacturing graphite, the raw petroleum coke is first calcined in large rotary or shaft kilns to shrink it and to drive out the volatile content. It is then broken down by crushers and mills and sized into a series of carefully controlled fractions through screens. The finest fraction, termed coke "flour", will have a maximum particle size of 0.015 inch for most electrode and specialty graphites while the coarsest fraction will have particles as large as 0.5 inch. In normal manufacture, selected size fractions are recombined to produce a dry aggregate with the sizes proportioned to yield the desired final properties.

The properly sized petroleum coke is then combined with coal tar pitch to make a plastic mix which is formable. This step in the process is usually carried out in large heated mixers. The carbonaceous mix is then ready to be formed to shape. The most common forming methods are extrusion and molding, both of which have several modifications. Most electrodes and metallurgical-type carbon and graphite articles are made by extruding the plastic mass using a hydraulic press and forcing the warmed material through a die. Conventional or closed-cavity pressure molding is used on most small shapes and some of the larger specialty and metallurgical shapes.

The next processing step is coking the pitch binder in formed pieces to develop an infusible carbon bond. This is done by bringing the product to a temperature of 750-900°C in a gas-fired furnace. The pieces must be carefully arranged and spaced , and tightly surrounded by a granular packing material since the binder liquifies in the early stages of the bake and the product becomes plastic. Very large furnaces are commonly used for baking where a high degree of control or property uniformity is not necessary. These furnaces range in size from 35,000 to 200,000 pounds product capacity, and baking cycles from 30 to 72 days are not unusual. In the course of baking, approximately one-third of the pitch binder is driven off through destructive distillation, which results not only in a loss in density but the development of porosity in the product.

The final step in graphite manufacture is the conversion of carbon to graphite in electric furnaces of the type originally employed by Acheson. This is known

Manuscript released by the authors September 1961
for publication as a WADD Technical Report.

as graphitizing and requires a temperature in the 2600-3000°C range. Total cycle time is 15 to 30 days, of which 2 to 6 days are heating and the remainder cooling. In graphitization, the graphite crystals, already present in random arrangement in the baked carbon piece rearrange in an ordered pattern of stacked parallel planes. This is accompanied by an abrupt change in the physical properties of the material as it transforms from carbon to graphite in situ. Commercial graphite produced in this manner contains as much as 30 per cent porosity and the degree of uniformity attained is usually dictated by economic considerations.

Since the early days of the carbon and graphite industry, various methods have been investigated and employed to produce high density graphite. In most of this work the ultimate goal was to obtain an artificial graphite having a density approaching that of a single crystal of graphite; namely, 2.26 gm/cm^3, as contrasted to normal manufactured graphite densities of 1.4 to 1.8 gm/cm^3. The course of research and development along this line followed, for the most part, what are now considered "conventional" processing techniques and were based on reducing the porosity of the article by means of filling the pores with a carbonaceous, and subsequently graphitizable, impregnant, or by adding to the green mix, fine particles of coke or carbon black to fill voids which would otherwise exist between the larger particles. Pitch impregnation of carbon articles prior to graphitization was patented in 1909[1] and has been a standard procedure in the manufacture of graphite since that time. The process for increasing density is not specifically claimed in this patent; however in 1912 a patent was issued which covered this point[2]. Multiple pitch impregnation has been used by National Carbon Company in attaining a density of 1.90 gm/cm^3 on a cylinder of graphite 48 inches in diameter by 84 inches long. This density was achieved by pitch impregnating the piece five times with a graphitization following each impregnation. For example, densities as high as 2.00 gm/cm^3 have been attained in the laboratory using the newer base grades of graphite and experimental impregnants.

The addition of fine particles to the green mix was investigated by National Carbon researchers as early as 1931, and since that time has been the subject of numerous investigations[3]. The use of furnace blacks in petroleum coke mixes has resulted in densities as high as 1.91 gm/cm^3; however, "making larger sizes of graphite of this density by the inclusion of furnace black is very difficult because of the problems involved in processing stock of such low permeability, but work is progressing in this direction"[4]. This work is also handicapped by the low thermal shock resistance of carbons containing furnace black.

The attainment of high density graphite is in itself no great accomplishment unless accompanied by an enhancement of other physical properties. Properly sized natural graphite, or graphite precipitated by the decomposition of carbides, can be easily molded to densities of above 2.10 gm/cm^3; however, because of the laminating tendency of natural graphite, the size of the molded article is limited to relatively small thickness, i.e., the dimension parallel to the pressure axis. The extreme weakness of molded natural graphite, especially in the "across the grain" direction, and its inherent "softness" makes this material almost totally unsuitable for an engineering material.

In the above methods (many more schemes have been tried with varying degrees of success) for producing high density graphite, there is little if any control over the structure of the graphite. The most practical, and widely used, method for producing high density graphite with higher strengths, lower permeability and resistivity, etc. is that of impregnation; however, during the course of the densification the basic structure of the article remains largely unchanged and only the porosity is decreased. The anisotropy present in the carbon or graphite article as determined by the initial forming step (molding or extrusion) remains throughout subsequent densification almost unchanged.

It was not until 1936, when Mr. V. C. Hamister, at the National Carbon Research Laboratory, demonstrated in a series of experiments that graphite stock was plastic when heated to high temperatures that the basis for a more radical and unique approach to the production of high density graphite was founded. In 1937, Mr. J. Gartland, at the same laboratory, showed that "gas baked coke stock was far more plastic than the resultant graphite and that this plastic range commenced at a lower temperature, when graphite is not plastic under the pressure used." Gartland stated later (1944) that the plasticity of carbon is "at least double that of graphite." Although Gartland pointed out that gas-baked carbon had higher plasticity than graphite, he apparently never considered hot working of carbon to obtain high density graphite, and the concept lay dormant until the nuclear and missile industries began to demand "super" graphites and the work was resumed at the National Carbon Research Laboratory by Mr. E. L. Piper in 1956.

Starting with a carbon sample 3/8" diameter x 1" long, having a bulk density of 1.56 gm/cm^3, Piper successfully processed this material in a makeshift arrangement to a density of 2.06 gm/cm^3. Because of the small size of this sample and the fact that it was treated as a curiosity (this is believed to be the highest density artificial graphite ever produced up until that time) its properties were not studied.

2. CREEP PROPERTIES OF CARBON AND GRAPHITE

The demonstrations of the plasticity of carbon and graphite at elevated temperatures by Hamister and Gartland formed the basis for the development of high density graphite by hot forming; however, it was necessary to investigate this phenomenon more closely in order to provide the necessary information for engineering design. While many of the high temperature physical properties of carbon and graphite can be roughly estimated from room temperature properties by experimentally determined relationships, this is not true of creep. Furthermore, there is no evidence that any room temperature property or combination of properties furnish any index of what the creep rate might be[5]. Therefore, to obtain meaningful data, the actual measurements had to be carried out at high temperatures.

No attempt will be made to present a detailed study of creep in carbon and graphite; however, since it forms the basis for the production of high density graphite by hot forming, some discussion of its application to the process is warranted.

The creep rate of carbon and/or graphite is dependent upon a number of factors such as (1) difference in base stocks; (2) temperature; and (3) load.[6,7] Graphite, being an anisotropic material, exhibits different creep rates with and across the grain. It is also generally accepted that graphite stocks containing larger particles exhibit higher creep rates than finer grain graphites, and that the creep rates are associated with factors such as pore structure, amount of binder coke, and others; however, these relationships are not fully established and understood. While it was well established that the plasticity (creep rate) of graphite increases with temperature, thus calling for the highest possible processing temperature in the case of this material, the plasticity characteristics of carbon seemed to be different from those of graphite and there was some reason to believe that there was a certain temperature at which optimum plasticity conditions prevailed. This expectation on one side and an undoubted plasticity increase with temperature due to temperature activation on the other led to the hypothetical plasticity curves for carbon as shown in Figure 1. Curve A indicates the

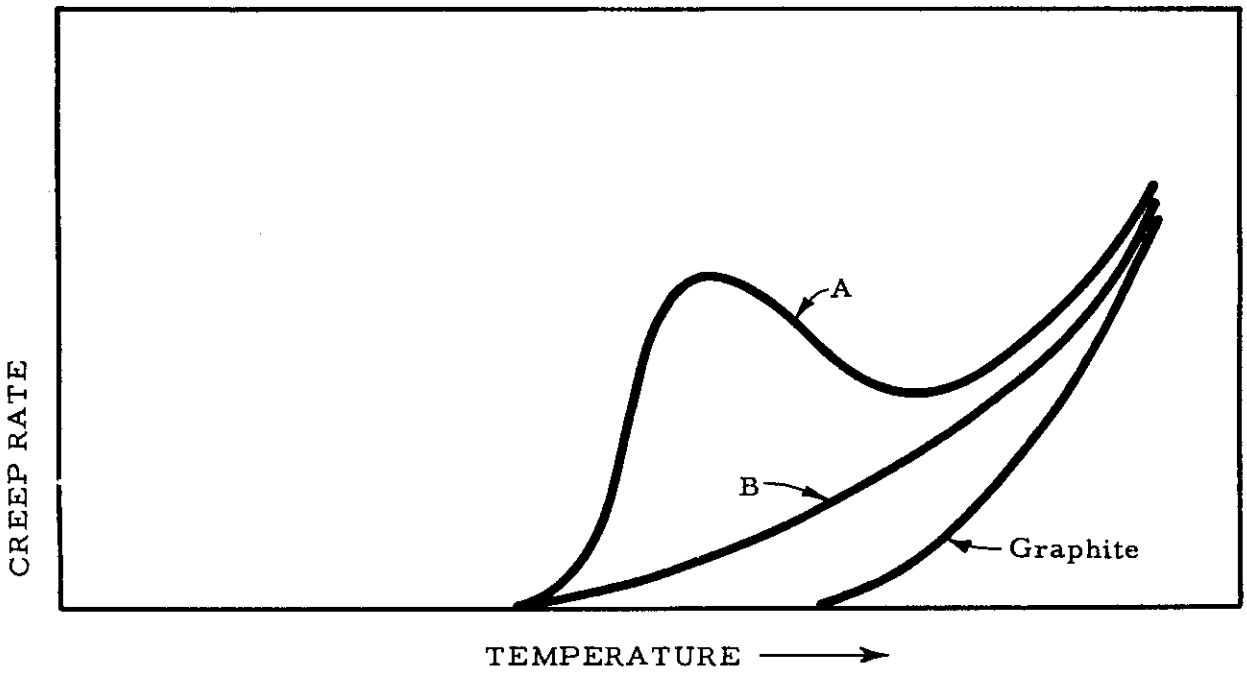

Figure 1. Hypothetical Creep Rates of Carbon as Function of Temperature.

hypothetical phenomenon of optimum plasticity of carbon by a plasticity peak below graphitization temperatures. Curve B, the equally probable and more likely assumption that the plasticity of carbon simply commences at a lower temperature and is thus larger than that of graphite, and Curve C shows the well known plasticity curve for graphite. If the first hypothesis were true (Curve A), the hot working process would be accomplished most effectively at the temperature of the plasticity peak.

With this in mind, the plasticity (creep under tension) of carbon and its graphitized allotrope was studied as a function of temperature according to the method of Stieber and Stroup.[5] The temperature range selected was 1200 to 2600°C. Figures 2 and 3 show creep vs. time curves for the various temperatures studied.

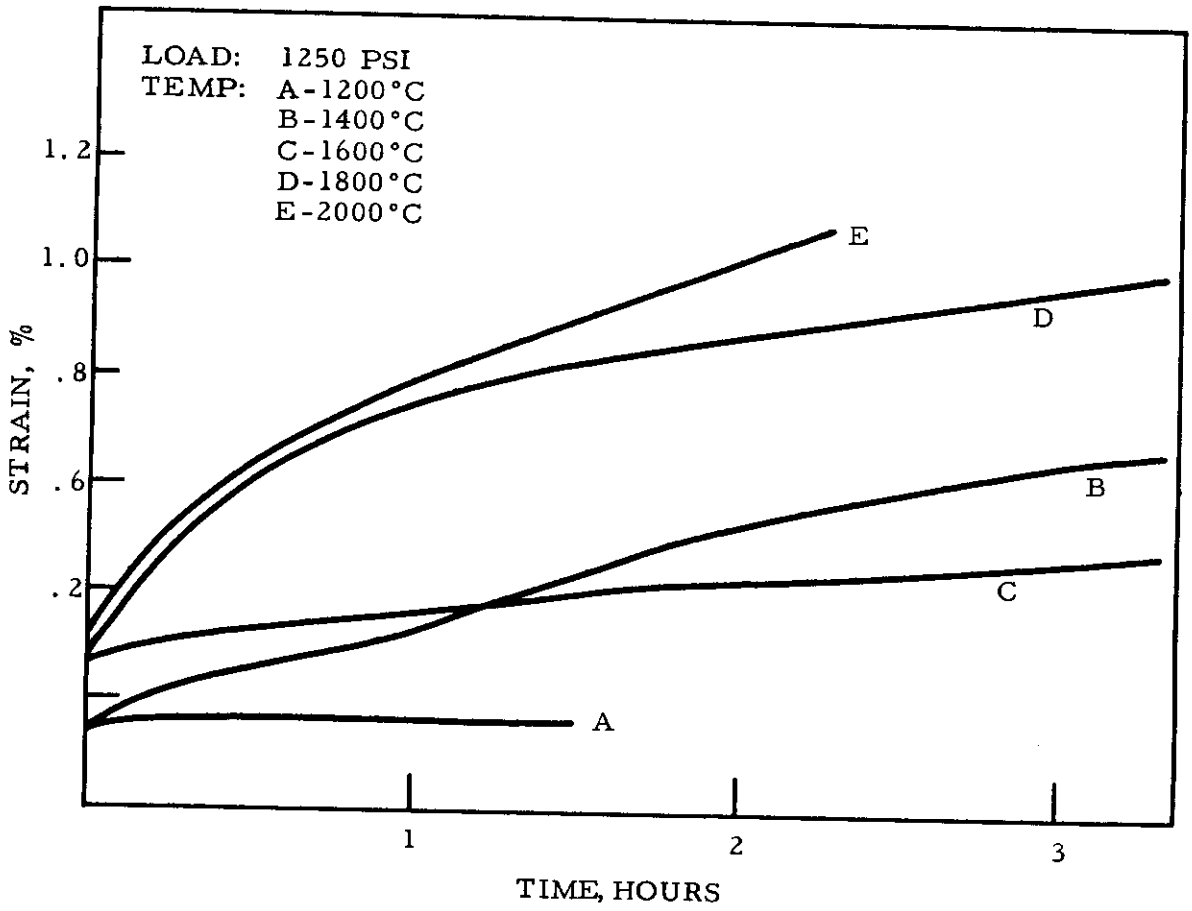

Figure 2. Creep of Carbon and Its Graphitized Allotrope from 1200°C to 2000°C.

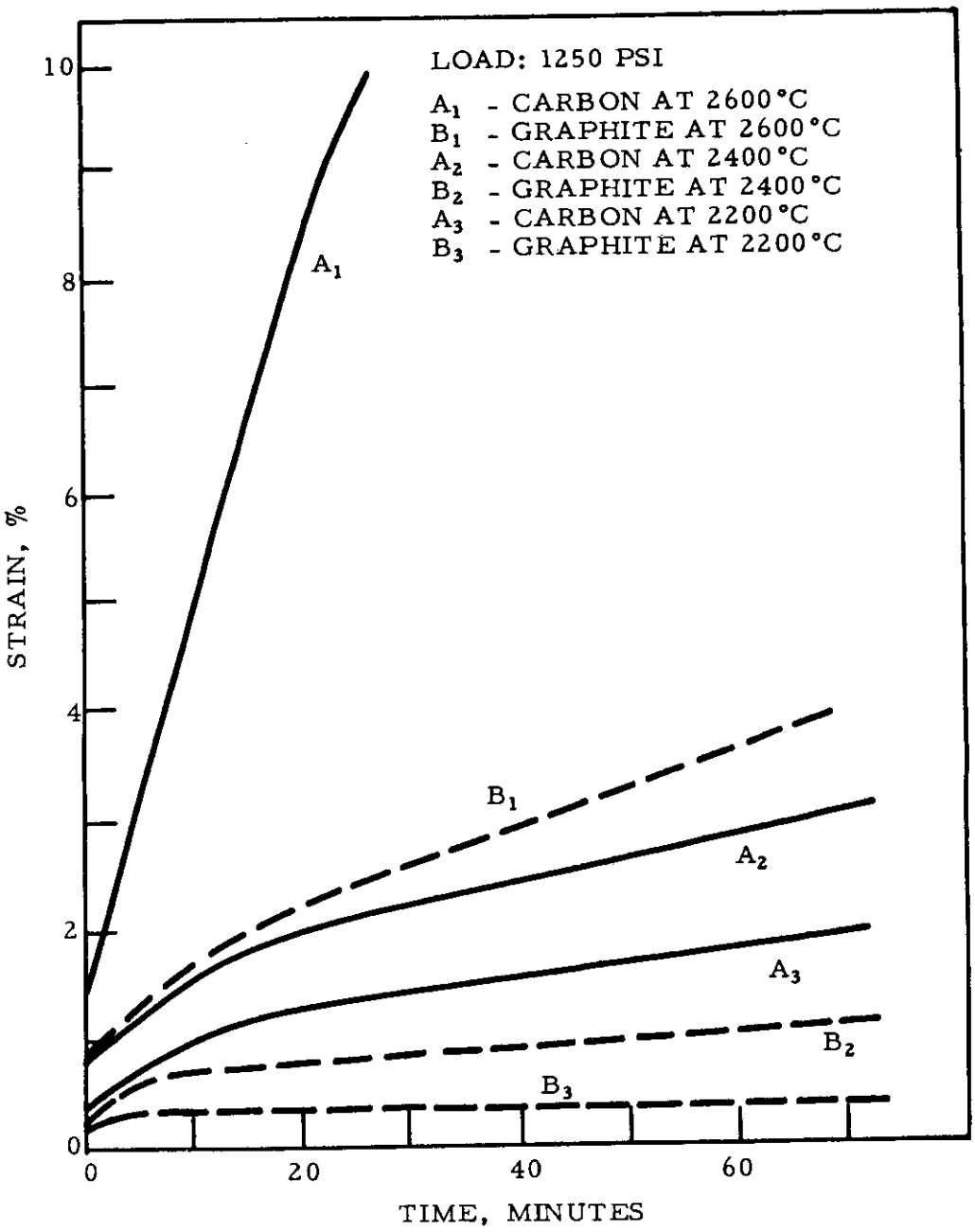

Figure 3. Creep of Carbon and Its Graphitized Allotrope from 2200 to 2600°C.

Of particular interest was the creep rate of carbon at 1400°C. At this temperature the creep rate appeared to be higher than 1600°C; however, the magnitude of the

increase in creep rate at 1400°C hardly fits in the category of a plasticity "peak", and it is insignificant when compared to the creep rates of carbon above 2400°C. Figure 4 shows the "steady state creep rate" vs. temperature for both carbon and

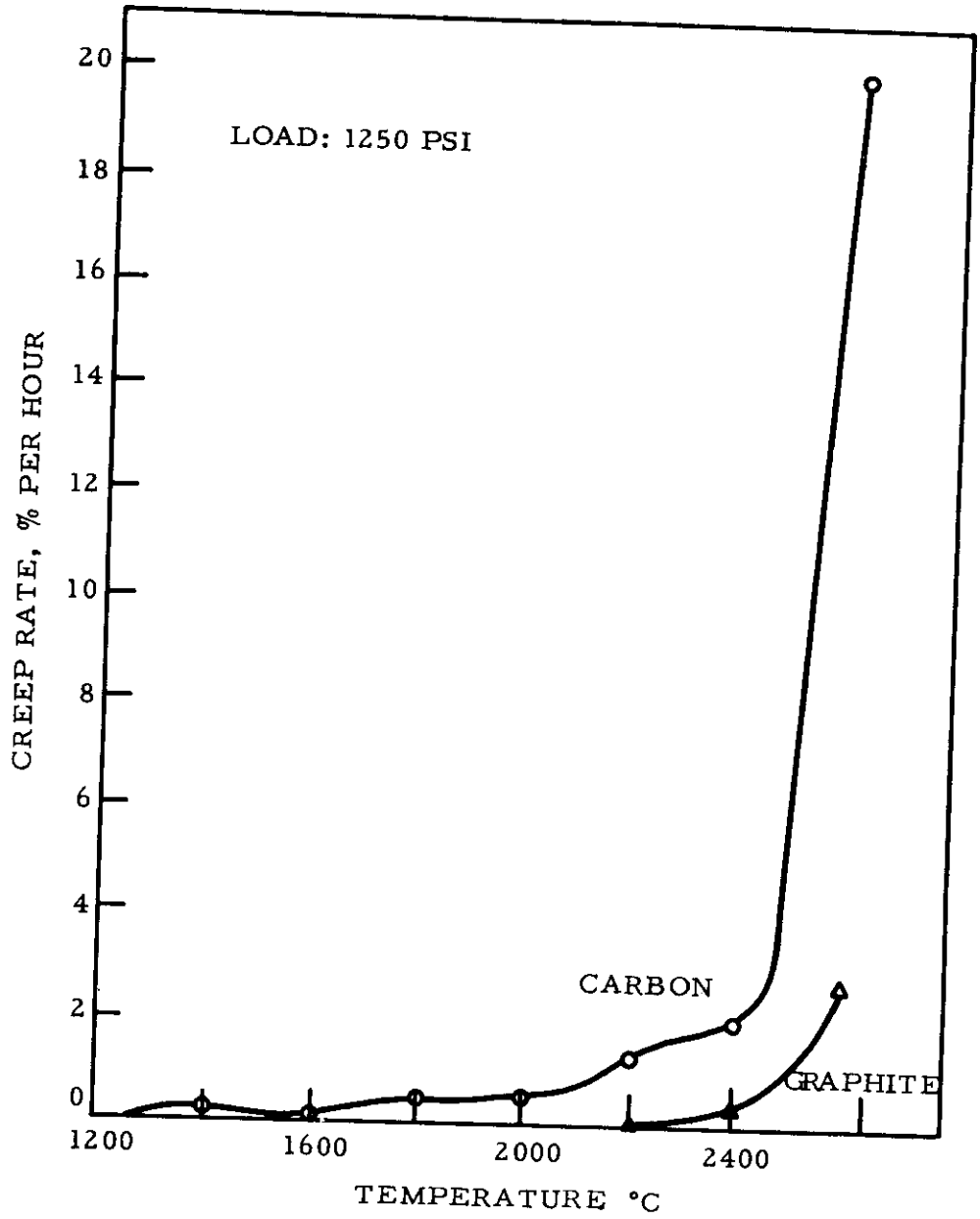

Figure 4. Creep Rate of Carbon and Its Graphitized Allotrope from 1200 to 2600°C.

graphite. Comparison of equivalent curves for carbon and its graphitized allotrope show the former to be outstandingly more plastic than the latter at high temperatures. This investigation was not extended to temperatures above 2600°C, since in that range considerable graphitization effects start to change the carbon as a function of time, which introduces further variables such as heating rate and hold period before applying the load.

The knowledge of the plasticity characteristics of carbon and graphite at high temperatures provided the background for obtaining a manufactured graphite with heretofore unattainable physical properties.

The process for the manufacture of high density (ZT) graphite can be stated very simply, i.e., carbon or graphite bodies are heated to a temperature at which they become plastic and are then compressed by the application of mechanical pressure. In practice, however, the process is far from simple because of the extremes of temperature and pressure needed to attain the necessary plasticity conditions. Two separate and distinct processes for the manufacture of high density graphite by hot working were developed based on proprietary processes of National Carbon Company. The hot working of graphite accomplishes more than densification - it results in a recrystallized highly oriented graphite intermediate in properties between standard commercial premium graphites and the pyrolytic and single crystal graphites.

3. PHYSICAL PROPERTIES OF HIGH DENSITY (ZT) GRAPHITE

3.1 Physical Properties of Initial Series of Hot Worked Graphite (ZT-X001)

The ZT-X001 series of graphites is produced by the hot working of a fine grain prefabricated commercial graphite. Of the numerous varieties of ZT graphite developed, this series has been the most exhaustively studied. This was primarily because of the early interest in this material by missile contractors for rocket nozzles and other components subjected to extreme temperature and stress conditions. Because of this interest, considerable effort was expended during the course of the development on obtaining physical properties sufficient to fully characterize this material. Emphasis was placed on both room temperature and elevated temperature properties. These properties were then correlated, whenever possible, to the actual performance in rocket motors.

The structure of ZT-X001 graphites is the finest known. Figure 5 shows a photomicrograph of ZT-5001 before and after hot working. Magnification is ~ 250X. The decreased porosity, and pore size, of ZT-5001 is quite evident from these photomicrographs, and the decrease is even more striking when one remembers that the starting material is one of the finest grain commercial graphites produced.

After Processing

Before Processing

Figure 5. Microstructure of ZT-5001 Graphite Before and After Processing - Magnification 250X.

Of particular interest was the change in physical properties with the change of bulk density. Four parameters - electrical resistivity, modulus of rupture, sonic modulus, and coefficient of thermal expansion - have been investigated for six members of the ZT-X001 family as a function of density. These results are shown graphically in Figures 6, 7, 8 and 9. The values shown here

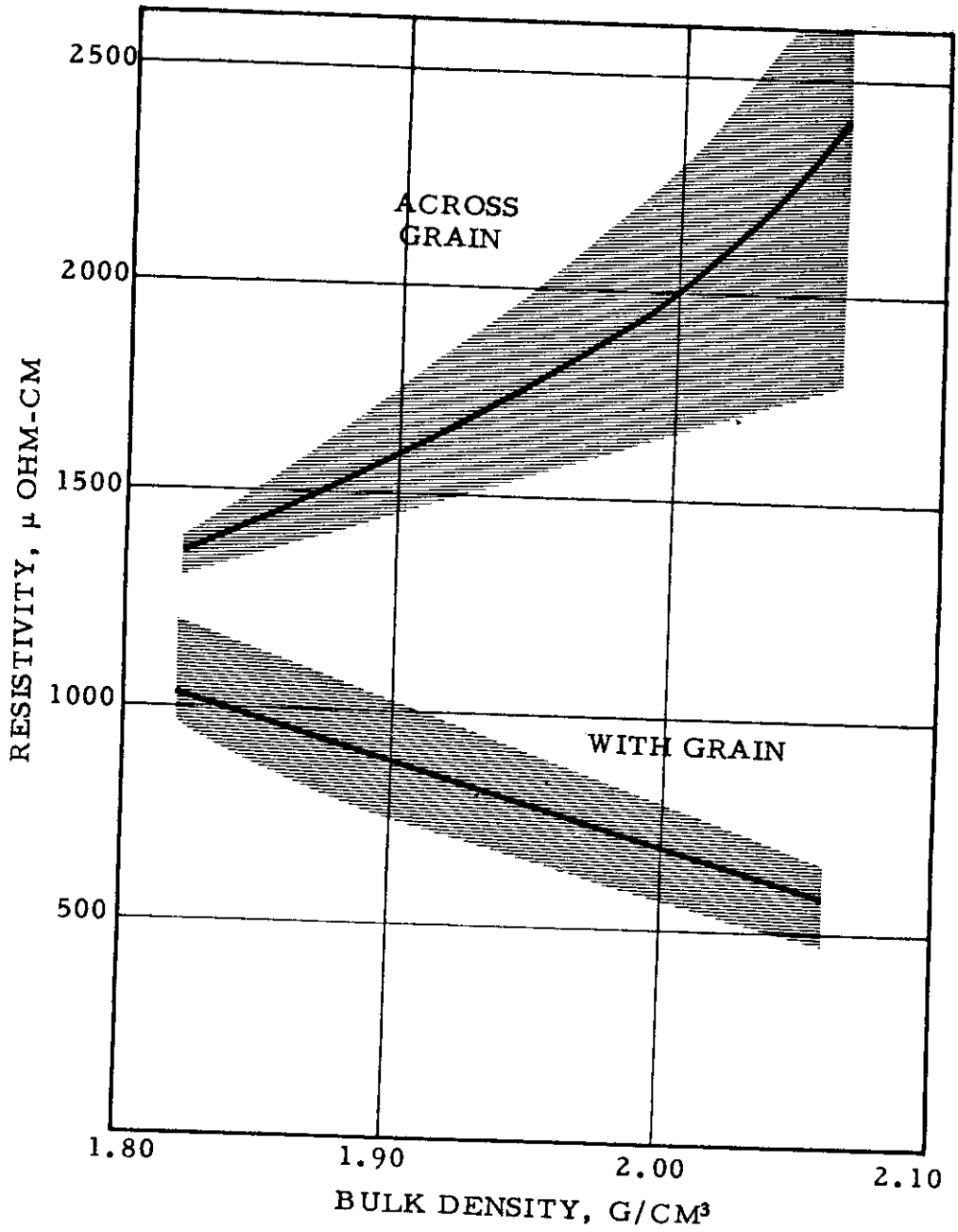

Figure 6. Electrical Resistivity of ZT-X001 Graphite vs Bulk Density.

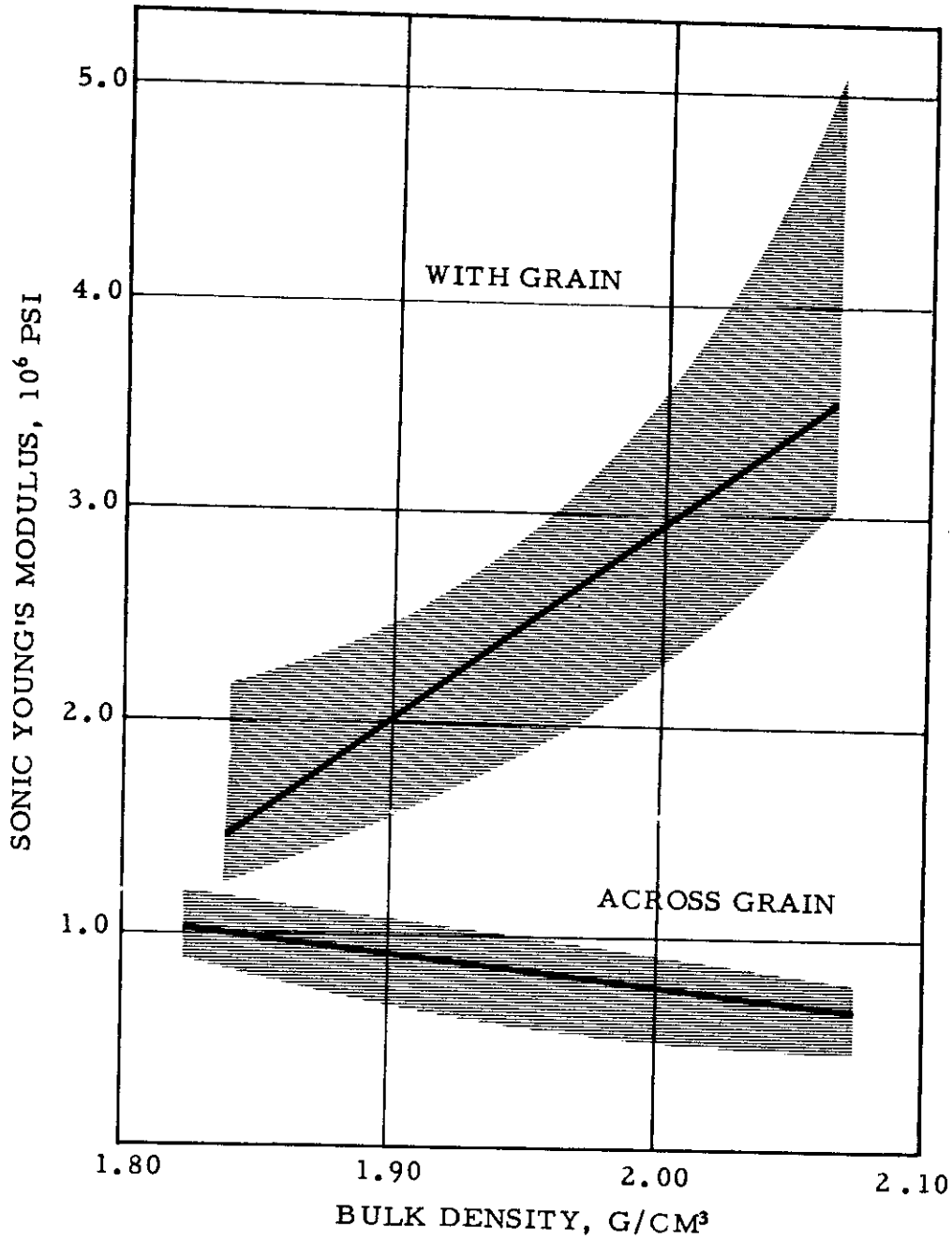

Figure 7. Young's Modulus (Sonic) of ZT-X001 Graphite vs Bulk Density.

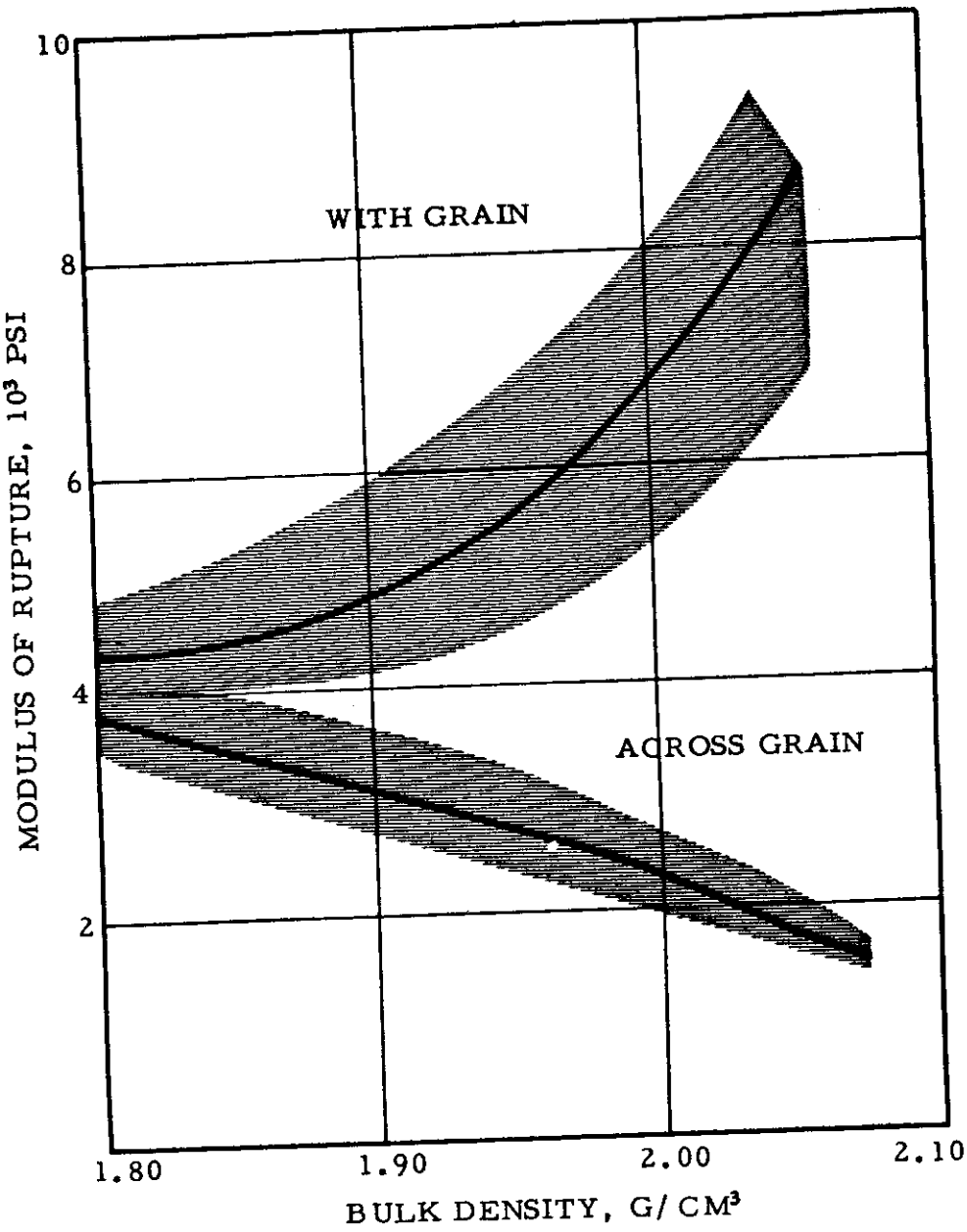

Figure 8. Modulus of Rupture of ZT-X001 Graphite vs Bulk Density.

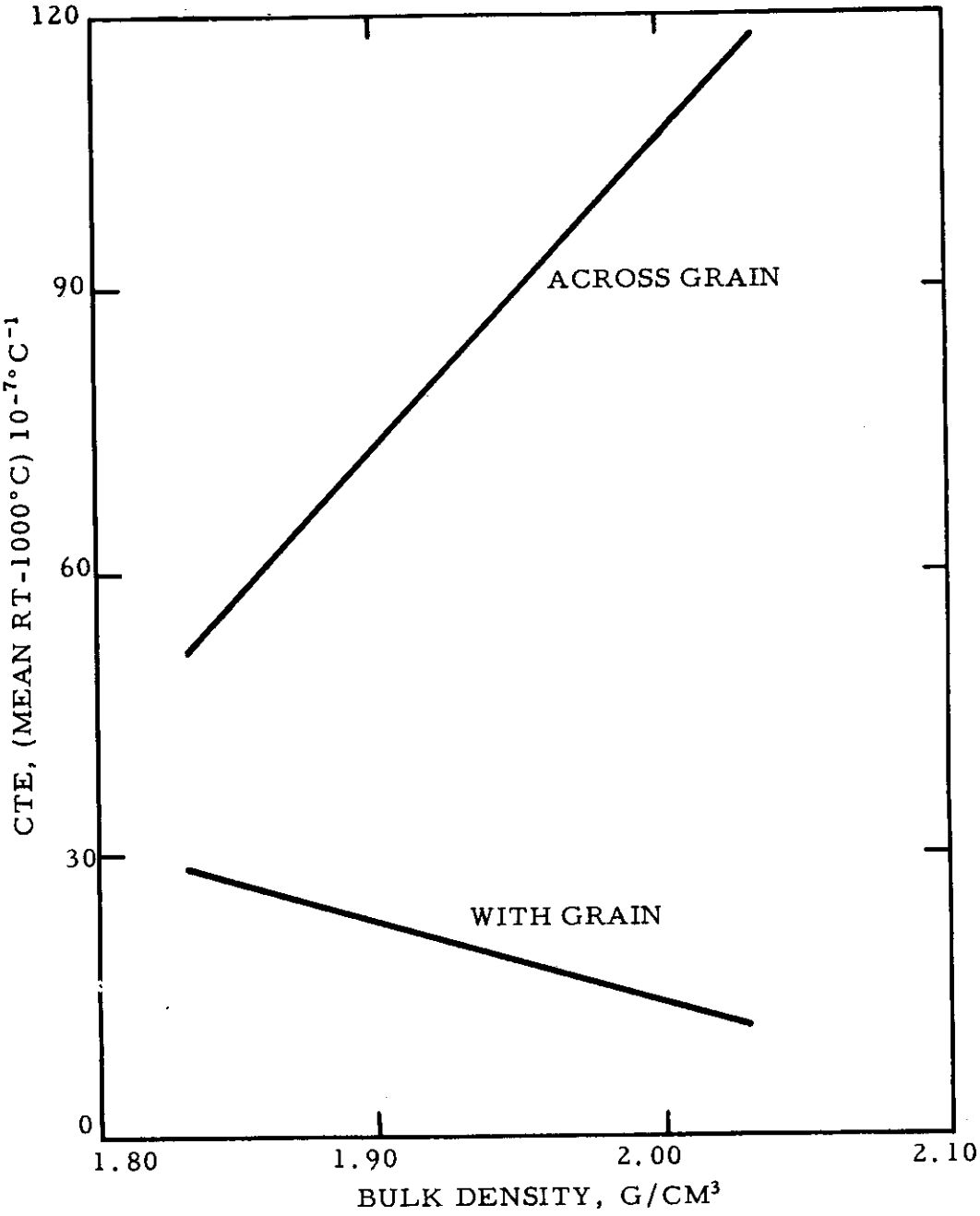

Figure 9. Coefficient of Thermal Expansion of ZT-X001 Graphite vs Bulk Density, Average from Room Temperature to 1000°C

are the average of forty to fifty individual determinations. These data, showing the average value and range of values for each density level, are given in Tables 1-4. The range in this case is between the actual maximum and minimum values, not a statistical limit. Also given in these tables are the anisotropy ratios of each property, i.e., the ratio of average across-grain to with-grain values.

Table 1. Specific Resistance (μ ohm-cm) of ZT-X001 Graphite

Grade	Ave. B.D. g/cm³	With Grain		Across Grain		Anisotropy Ratio
		Ave.	Range	Ave.	Range	
ZT-1001	1.82	1050	950 - 1200	1350	1300 - 1450	1.29
ZT-2001	1.87	920	770 - 1070	1500	1400 - 1630	1.63
ZT-3001	1.92	850	680 - 980	1670	1500 - 1900	1.97
ZT-4001	1.97	750	600 - 850	1860	1600 - 2150	2.48
ZT-5001	2.02	650	510 - 700	2100	1680 - 2480	3.24
ZT-6001	2.07	580	450 - 630	2550	1900 - 3000	4.40

Table 2. Sonic Young's Modulus (10^6 psi) of ZT-X001 Graphite

Grade	Ave. B.D. g/cm³	With Grain		Across Grain		Anisotropy Ratio
		Ave.	Range	Ave.	Range	
ZT-1001	1.82	1.40	1.20-2.13	1.05	0.87-1.20	1.33
ZT-2001	1.87	1.70	1.40-2.26	0.95	0.77-1.12	1.79
ZT-3001	1.92	2.20	1.77-2.36	0.85	0.67-1.03	2.59
ZT-4001	1.97	2.65	2.12-3.27	0.77	0.55-0.94	3.44
ZT-5001	2.02	3.15	2.67-4.26	0.68	0.47-0.87	4.63
ZT-6001	2.07	3.60	3.16-5.68	0.60	0.42-0.83	6.00

Table 3. Modulus of Rupture (psi) of ZT-X001 Graphite

Grade	Ave. B.D. g/cm³	With Grain		Across Grain		Anisotropy Ratio
		Ave.	Range	Ave.	Range	
ZT-1001	1.82	4500	3850- 5000	3600	3200-4050	1.25
ZT-2001	1.87	4700	3950- 5600	3300	2850-3700	1.42
ZT-3001	1.92	5300	4200- 6300	3000	2500-3400	1.77
ZT-4001	1.97	6000	4900- 7300	2600	2150-3050	2.31
ZT-5001	2.02	7500	6150- 8750	2200	1800-2450	3.41
ZT-6001	2.07	9800	7700-10,500	1700	1450-1950	5.75

Table 4. Coefficient of Thermal Expansion (10^{-7} °C^{-1}) of ZT-X001 Graphite*

Grade	Ave. B.D. g/cm³	Linear Expansion With Grain Average	Linear Expansion Across Grain Average	Anisotropy Ratio	Volume Expansion Average
ZT-1001	1.82	28.5	52.0	1.82	109.0
ZT-2001	1.87	25.0	69.5	2.78	119.5
ZT-3001	1.92	21.5	85.0	3.95	128.0
ZT-4001	1.97	18.0	102.	5.67	138.0
ZT-5001	2.02	15.0	119.	7.95	149.0
ZT-6001	2.07	12.0	135.	11.23	159.0

*Mean coefficient of expansion from room temperature to 1000 °C.

The data for resistivity, Young's Modulus, and modulus of rupture are from measurements at room temperature. The data for coefficient of thermal expansion, however, are mean values from room temperature to 1000 °C.

These data were of value in several respects. The change in physical properties with density was defined, and the degree of variation at the various density levels was established. It is to be noted that the properties of the ZT-X001 graphites show the effect of increased orientation with increased density, and that these properties are progressing closer to single crystal properties with increasing density. It should also be noted that the range in properties will be greater in the higher density materials; however, its magnitude is not truly represented by the values shown. All of these data were taken on material produced during the period of process experimentation and reflect the wide variations in processing conditions being employed at the time.

3.2 Physical Properties of Grade ZTA Graphite

Grade ZTA was the first of the family of ZT graphites to be assigned a standard commercial grade designation and to be produced on a commercial scale. It was evolved from the ZT-X001 series and is presently manufactured in sizes up to 14 inch diameter by 10 inch long. Although manufacture of this material has been assumed, for the most part, by the National Carbon production organization, large quantities have been, and are still being, produced on laboratory equipment. The properties of ZTA discussed below include both laboratory and plant production, and include samples produced under widely varying conditions. It should, therefore, be noted that a standardized routine processing procedure was not in effect for the production of all material sampled; therefore, the overall property spread is greater than would be expected under standardized processing. Even under the conditions which existed during the production of the stock discussed here, it will be noted that the property spread of ZTA is considerably less than that of the most uniform standard commercial graphite previously produced.

3.2.1 Structure of ZTA Graphite

One of the problems that has plagued manufacturers and users of graphite for years has been the presence of internal flaws undetectable by normal inspection procedures. Since grade ZTA has been developed for extremely critical applications where even minute structure malformations cannot be tolerated, it is essential that this material be rigorously inspected to assure complete freedom from flaws. For this reason, all ZTA graphite is subjected to a thorough X-ray examination before being released for shipment. Any evidence of laminations, voids, or wide density variation within the piece is reason for rejection. The importance of this X-ray examination to the users of ZTA graphite is borne out by the results on the most recent ZTA production as shown in Table 5. The cause for rejection in most pieces was small internal cracks which would have passed undetected, except for X-ray inspection.

Table 5. X-Ray Inspection Results on ZTA Graphite

Size	No. Inspected	No. Rejected	No. Accepted	Yield %
8-1/2" dia.	47	1	46	97.9
14" dia.	101	11	90	89.1

X-ray examination has been used extensively during the course of ZTA process development. Its value can best be illustrated by referring to the results tabulated above. Of the eleven rejected 14 inch diameter pieces, six occurred in succession. Upon checking the processing records of each piece, it was found that a minor change in the process had been made at the time the rejected pieces were formed. This point in the process cycle was then corrected, and subsequent production proceeded with practically no scrap.

3.2.2 Bulk Density of ZTA Graphite

The bulk density limits of ZTA graphite were established to be 1.92 to 1.97 gm/cm^3 measured on the full size piece. Any material having a density above or below these limits is not designated as ZTA. This density specification has necessitated the measurement of each piece of ZTA produced, from which considerable data have been compiled. The average bulk density and standard deviation for the sizes of ZTA produced to date have been calculated, and these results, along with the average bulk density and standard deviation of National Carbon grade ATJ graphite for comparison are given in Table 6. Grade ATJ is an extremely fine-grain, essentially flaw free, premium quality graphite which has for some time been an accepted missile grade graphite. Prior to the introduction of ZTA graphite, ATJ was one of the highest quality graphites known.

Table 6. Average Bulk Density and Standard Deviation - ZTA Graphite

Grade	Size	No. of Samples	Average Bulk Density g/cm³	Standard Deviation
ATJ*	9 x 20 x 24"	--	1.730	.034
ZTA	4" dia. x 6" to 12" long	103	1.947	.017
ZTA	8-1/2" dia. x 11" long	31	1.944	.014
ZTA	14" dia. x 10" long	128	1.946	.014

*"The Industrial Graphite Engineering Handbook", National Carbon Company, Rev. 10/60, page 4.09.

Of equal importance to the reduction in variation from piece to piece is the degree of variation of density within the individual pieces. Figures 10 through 13

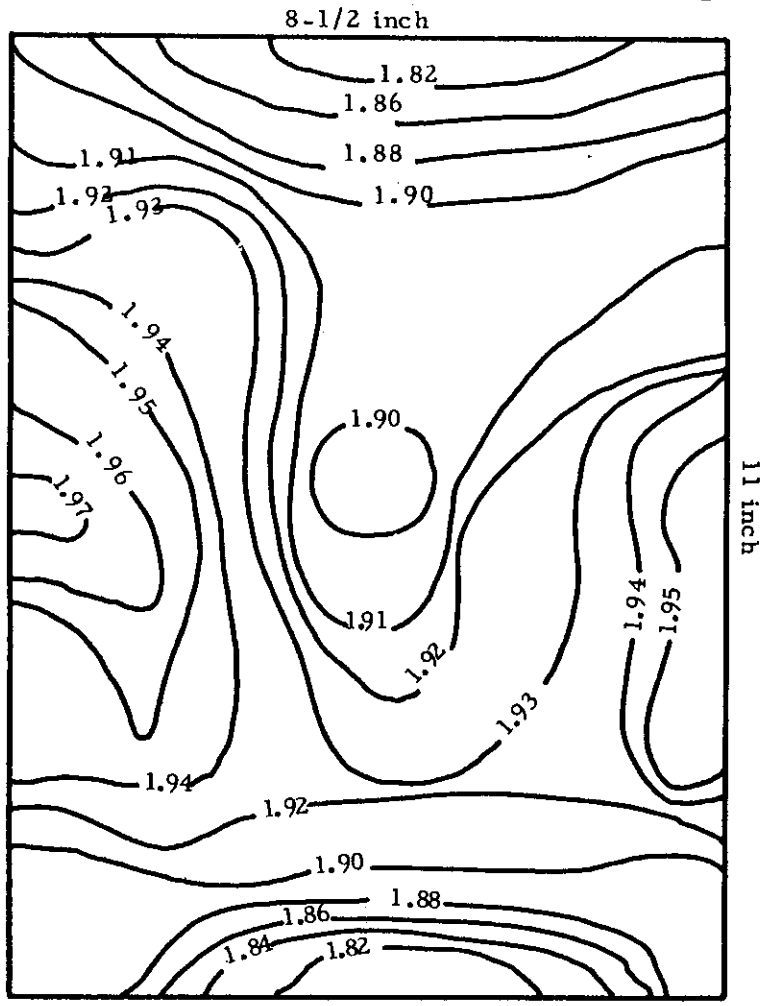

Figure 10. Bulk Density Profile, 8-1/2 inch Diameter ZTA Graphite, Piece 35.

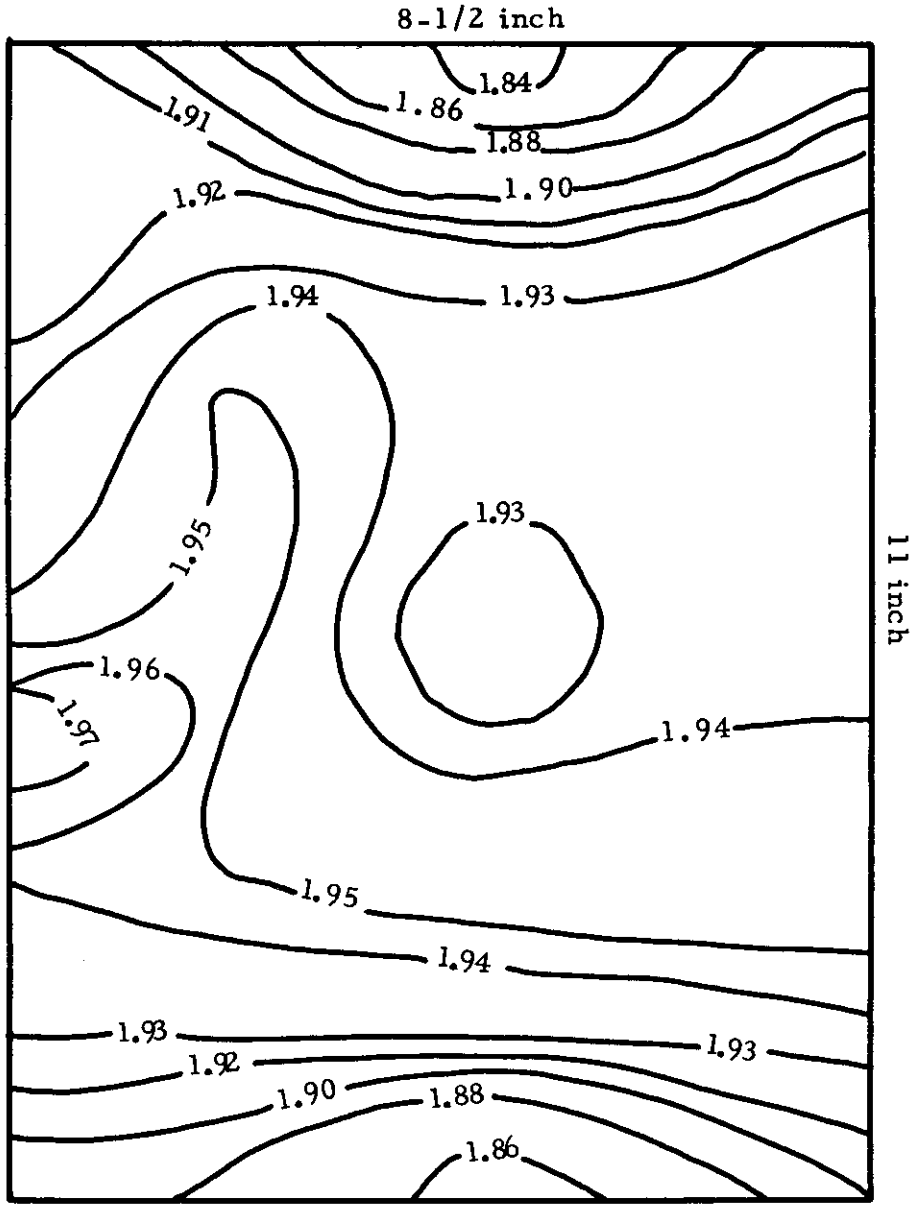

Figure 11. Bulk Density Profile, 8-1/2 inch Diameter ZTA Graphite, Piece 36.

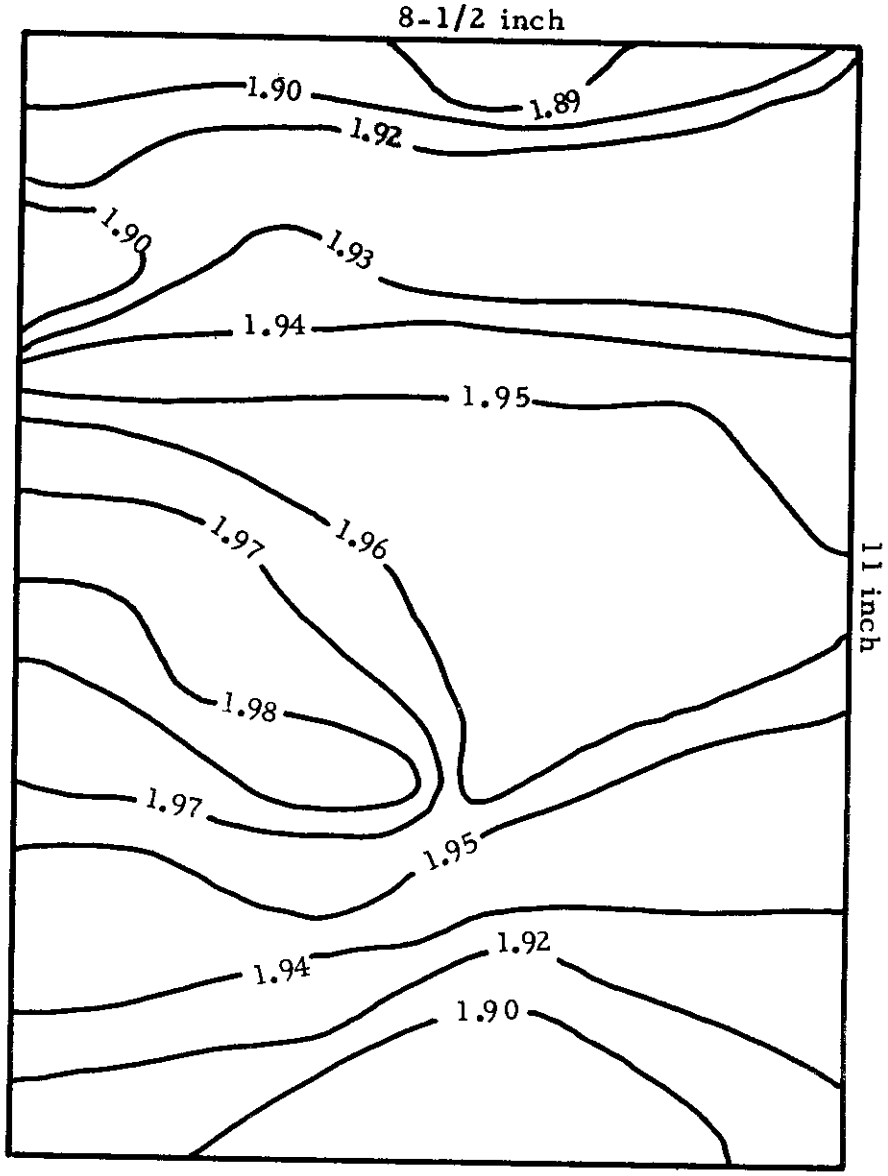

Figure 12. Bulk Density Profile, 8-1/2 inch Diameter ZTA Graphite, Piece 37.

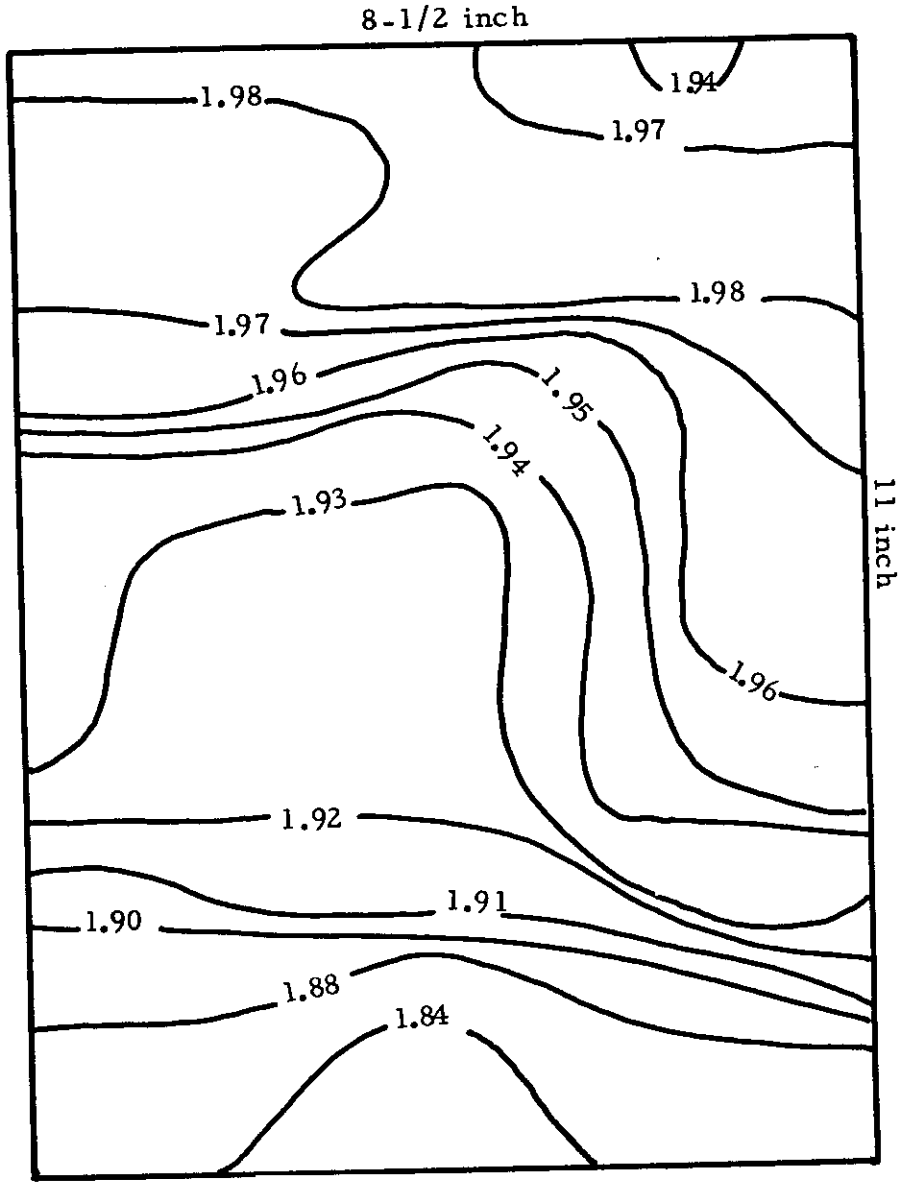

Figure 13. Bulk Density Profile, 8-1/2 inch Diameter ZTA Graphite, Piece 41.

show the density profiles of four pieces of 8-1/2 inch diameter x 11 inch long ZTA graphite. The generally lower density tops and bottoms are due to less plasticity in these areas during the hot working process, and consequently have not been compressed to the degree of the center section. Average density and standard deviation for each piece (8-1/2 inch dia. x 11 inch long) were calculated and are tabulated in Table 7. In addition, the average density and standard deviation were calculated for the same four pieces trimmed to 8-1/2 inch diameter x 9 inch long, i.e., one inch was removed from each end. These data, also given in Table 7, clearly show the effect on both the average density and standard deviation of removing the "non-ZT" portion of the piece. Improvements in processing equipment and techniques have now eliminated the low density ends as becomes evident from the more recent data on 14 inch diameter ZTA below.

Table 7. Bulk Density Variation Within 8-1/2 inch Diameter ZTA Graphite

Pc. No.	Size	No. of Samples	Avg. Bulk Density g/cm^3	Standard Deviation	Standard Deviation % of Avg.
35	8-1/2" dia. x 11" lg.	84	1.911	.037	1.94
35	8-1/2" dia. x 9" lg.	70	1.923	.024	1.25
36	8-1/2" dia. x 11" lg.	39	1.926	.030	1.56
36	8-1/2" dia. x 9" lg.	31	1.938	.015	.78
37	8-1/2" dia. x 11" lg.	42	1.943	.027	1.39
37	8-1/2" dia. x 9" lg.	38	1.949	.018	.92
41	8-1/2" dia. x 11" lg.	34	1.941	.033	1.70
41	8-1/2" dia. x 9" lg.	31	1.948	.024	1.23

The density profile of a piece of 14 inch diameter x 10 inch long ZTA is shown in Figure 14. Average density and standard deviation for two pieces are given in Table 8. From the density profile and the data in Table 8, it is obvious that the low density ends are absent and the density throughout the 14 inch diameter ZTA is somewhat more uniform. This should not be taken to mean that 14 inch diameter ZTA is necessarily more uniform than the 8-1/2 inch diameter stock, only that the data for 8-1/2 inch diameter ZTA are from earlier production.

Table 8. Bulk Density Variation Within 14 inch Diameter ZTA Graphite

Piece No.	No. of Samples	Average Bulk Density g/cm^3	Standard Deviation	Standard Deviation Per Cent of Average
N 23	108	1.967	.019	.97
20	104	1.937	.022	1.14

With the foregoing emphasis on uniformity, it should be pointed out that one of the objectives of Contract No. AF 33(616)-6915 was to reduce the variation within specific grades of graphite suitable for missile applications. The increased uniformity of grade ZTA represents the attainment of this objective; however, a

continued effort to further improve the uniformity of this material is in process.

3.2.3 Mechanical Properties of ZTA Graphite

The mechanical properties of ZTA graphite have been studied on representative samples of all sizes produced to date. Since the determinations of these properties are by destructive methods, the number of ZTA pieces sampled is necessarily more limited than in the case of average density; however, when compared to standard commercial graphite, the percentage is fairly high. The properties reported here are, for the most part, room temperature values. Table 9 gives a summary of the average value for these properties. Values for grade ATJ are included for comparison.

Table 9. Typical Room Temperature Mechanical Properties of ZTA Graphite

Property	Units	With Grain		Across Grain	
		ZTA	ATJ	ZTA	ATJ
Modulus of Rupture	lb./in.^{2}	5940	3320	2270	3330
Compressive Strength	lb./in.^{2}	8900	8330	11,400	8530
Young's Modulus	10^6 lb./in.^{2}	2.89	1.40	.73	1.15

Unfortunately, an insufficient number of ZTA pieces have been measured to permit the calculation of a completely reliable standard deviation for the properties tabulated in Table 9; however, work to this end is in progress. As an indication of the uniformity of ZTA, the variation of physical properties within ZTA piece No. 23N, the density profile of which is shown in Figure 14, can be described as follows. The standard deviations for the modulus of rupture are 9 per cent and 7 per cent for ZTA with and across the grain respectively vs 17 per cent and 15 per cent for ATJ. Similar reductions were evident for the other properties determined. These data are considered quite typical for ZTA graphite as currently produced.

The anisotropy of ZTA graphite is such that the ratios of with- to across-the-grain mechanical property values differ considerably from those of the more isotropic ATJ graphite. This is not unexpected since ZTA is intermediate in properties between ATJ and pyrolytic graphite. As an example, the values of Young's Modulus for ATJ, ZTA, pyrolytic and single crystal graphite are plotted vs bulk density in Figure 15. The modulus along the grain increases smoothly from 1.4 million psi for ATJ through ZTA to nearly 10 million psi for pyrolytic graphite, and to more than 100 million psi for the single crystal. The modulus across the grain decreases from ATJ to ZTA but appears to be higher for pyrolytic and single crystal graphite. The single crystal value across the grain is estimated to fall between 4 and 5 million psi and a single experimental determination obtained by the measurement of lattice vibration wave velocity on an unannealed piece of pyrolytic graphite was about one-third lower. These values need to be supplemented by additional studies.[8]

Unfortunately, work at the Advanced Materials Laboratory has not progressed, at the time of this writing, to the point where sufficient high temperature property values are available for an analysis; however, this work is in progress. Some data

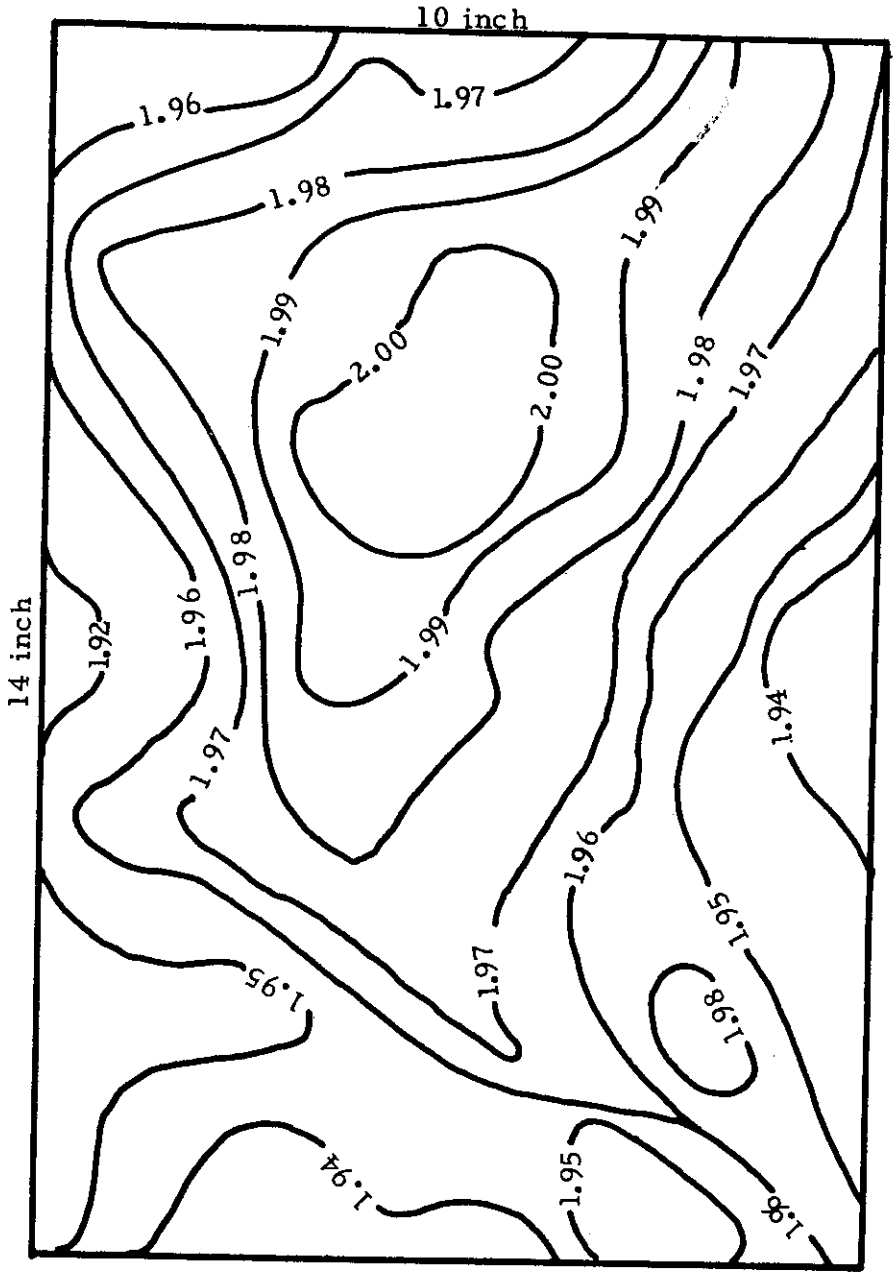

Figure 14. Bulk Density Profile, 14 inch Diameter ZTA Graphite, Piece 23N.

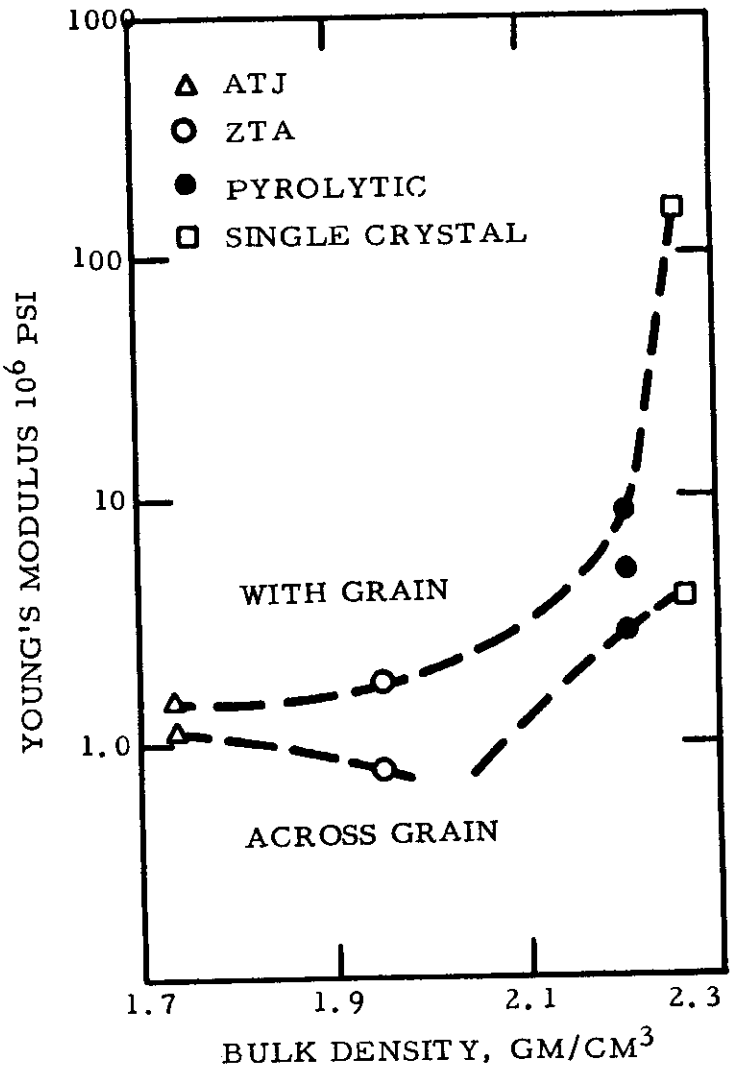

Figure 15. Young's Modulus for Various Graphites vs Bulk Density.

however, are available on the variation of Sonic Young's Modulus with temperature over the range from room temperature to 2000°C.

These data are plotted in Figure 16. Both ATJ and ZTA show increasing

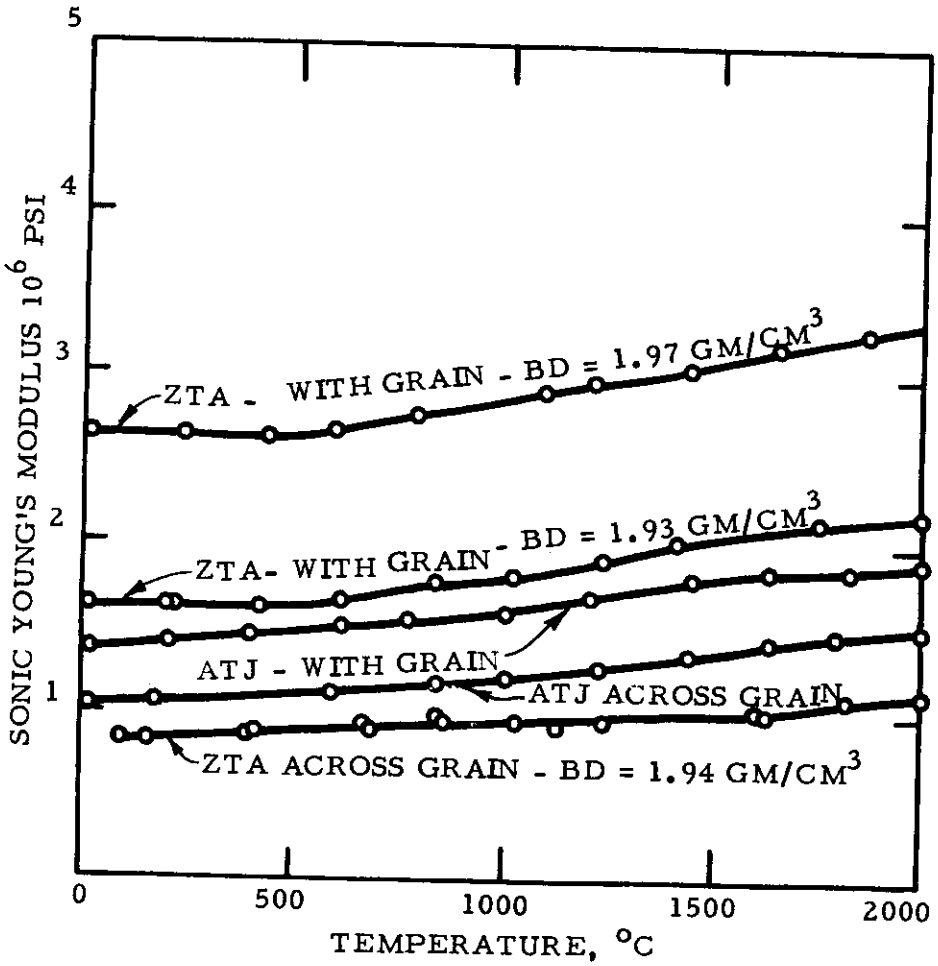

Figure 16. Sonic Young's Modulus of ZTA and ATJ Graphites vs Temperature.

Sonic Young's Modulus with increasing temperature, both along and across the grain. This behavior is also well known for the strength of polycrystalline graphite up to approximately 2500°C.

Through a sub-contract with Aeronutronic Division of Ford Motor Company, some data on the variation of ultimate tensile strength of ZTA and ATJ graphite with temperature are available. This work is incomplete and the results are preliminary. Data are given for ATJ, ZTA, and annealed (to 3000°C) ZTA in two directions (with and across the grain) for temperatures up to approximately 2600°C

(4750°F). The values for ATJ, as given in Tables 10 and 11, fall within the

Table 10. Temperature-Strength Data for ATJ Graphite Oriented Across Grain

Specimen No.	Temperature °C	Ultimate Tensile Strength psi
14	2380	4565
4	2260	4225
6	2200	3380
10	2010	3770
8	1715	4125
11	1620	4025
7	1592	3740
2	1440	3495
1	1092	3130
12	21	2935

Table 11. Temperature-Strength Data for ATJ Graphite Oriented With Grain

Specimen No.	Temperature °C	Ultimate Tensile Strength psi
1	2220	4565
14	2020	4025
17	1995	4990
3	1840	4065
10	1830	3395
9	1605	4395
4	1382	3480
13	1230	3380
5	830	3330
2	21	2630

variation limits of prior tests on like material. The values for ZTA, both annealed and unannealed, are given in Tables 12 through 15. These data are also shown graphically in Figures 17 and 18. From the tables and the plots of tensile strength vs temperature it will be noted that there is little if any difference between the annealed and unannealed ZTA specimens. The results plotted in Figures 17 and 18 show no clear evidence for a maximum in strength for ZTA graphite at high temperature. Other data obtained more recently have shown a maximum tensile strength in the neighborhood of 2500°C.

Table 12. Temperature-Strength Data for ZTA Graphite Oriented With Grain

Specimen No.	Temperature °C	Ultimate Tensile Strength psi
2-10	21	4045
2-18	1315	5410
2-22	1565	5250
2- 6	1680	5095
2- 2	1840	5985
2- 9	1985	7510
2- 1	2135	4900*
2- 8	2190	7350
2-15	2230	5600
2-14	2425	8115**
2-21	2450	7950
2-16	2480	7630
2-12	2490	6630
2- 5	2620	9295

* Load Rate = 0.200 inch/min.
** Load Rate = 0.002 inch/min.
All others: Load Rate = 0.020 inch/min.

Table 13. Temperature-Strength Data for ZTA Graphite Oriented Across Grain

Specimen No.	Temperature °C	Ultimate Tensile Strength psi
1- 2	21	1495
1- 4	1220	1210
1-18	1565	1530
1-22	1680	2390
1-17	1780	2480
1- 7	1935	1690
1- 8	2100	2070
1-23	2140	1180*
1- 3	2140	1050
1-11	2290	1780**
1-21	2350	1810
1-13	2375	2005
1-20	2450	2160
1-16	2450	1810
1-19	2560	1780

* Load Rate = 0.200 inch/min.
** Load Rate = 0.002 inch/min.
All others: Load Rate = 0.020 inch/min.

Table 14. Temperature-Strength Data for 3000°C Annealed ZTA Graphite Oriented Across Grain

Specimen No.	Temperature °C	Ultimate Tensile Strength psi
3-11	21	1180
3- 7	1310	1050
3- 1	1565	1240
3-12	1680	1750
3-19	1825	2035
3- 6	1980	1465
3- 2	2480	1750
3-14	2190	985*
3-15	2190	2325
3- 4	2220	1335
3-21	2325	1815
3-22	2350	1210*
3-20	2370	1400**
3-18	2445	1845
3-13	2565	1940

* Load Rate = 0.200 inch/min.
** Load Rate = 0.002 inch/min.
All others: Load Rate = 0.020 inch/min.

Table 15. Temperature-Strength Data for 3000°C Annealed ZTA Graphite Oriented With Grain

Specimen No.	Temperature °C	Ultimate Tensile Strength psi
4- 7	21	3535
4-14	340	4650
4-10	1570	3950
4-19	1680	5985
4-16	1815	6870
4-22	1935	7350
4- 8	2180	5635*
4- 2	2240	7955**
4- 9	2240	5890*
4- 6	2290	7990
4- 3	2340	8850
4-12	2440	7195
4-18	2465	6370
4- 5	2505	6420
4-15	2610	8275

* Load Rate = 0.200 inch/min.
** Load Rate = 0.002 inch/min.
All others: Load Rate = 0.020 inch/min.

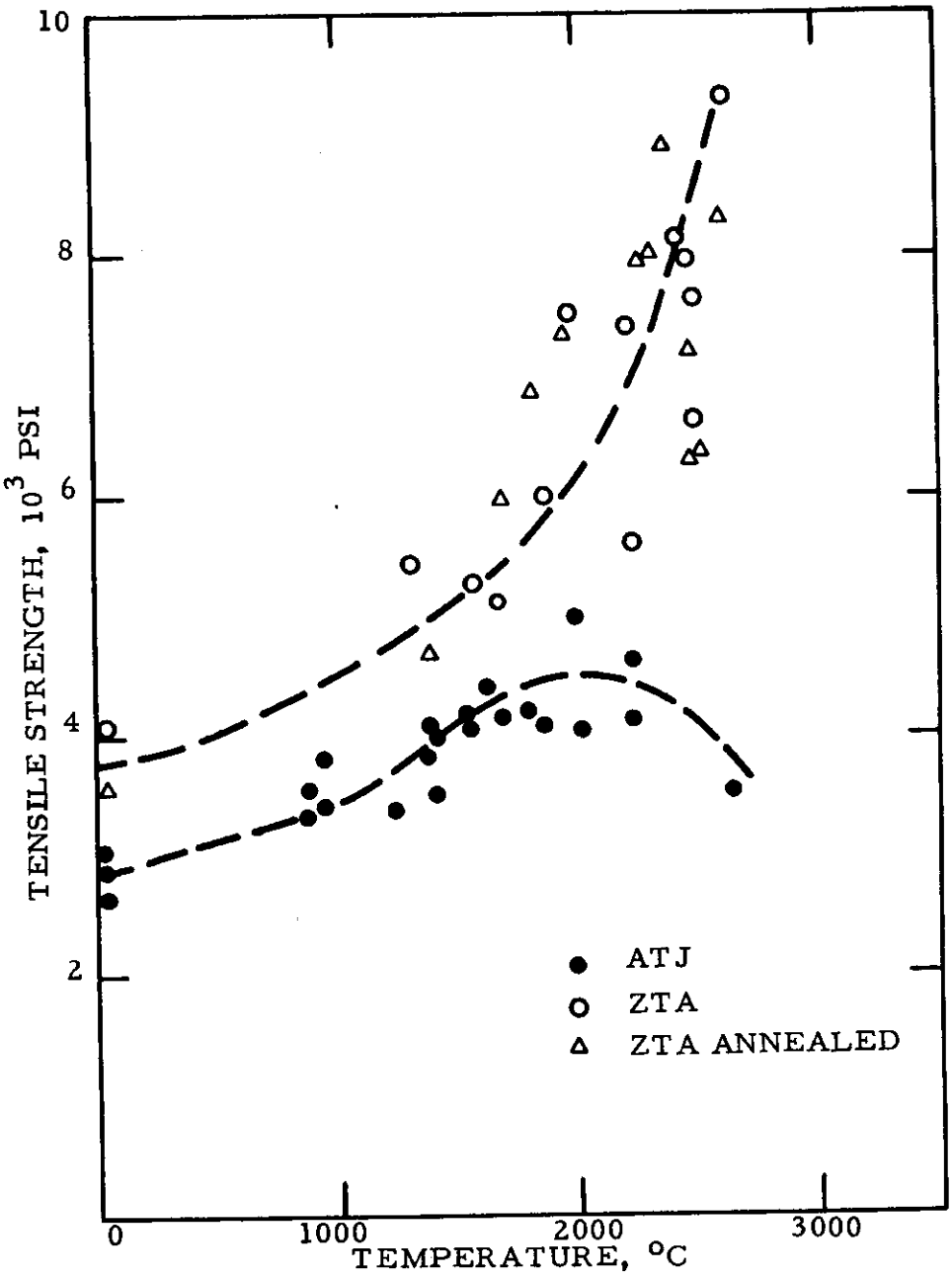

Figure 17. Short-time Tensile Strength vs Temperature -ZTA and ATJ Graphite - With Grain.

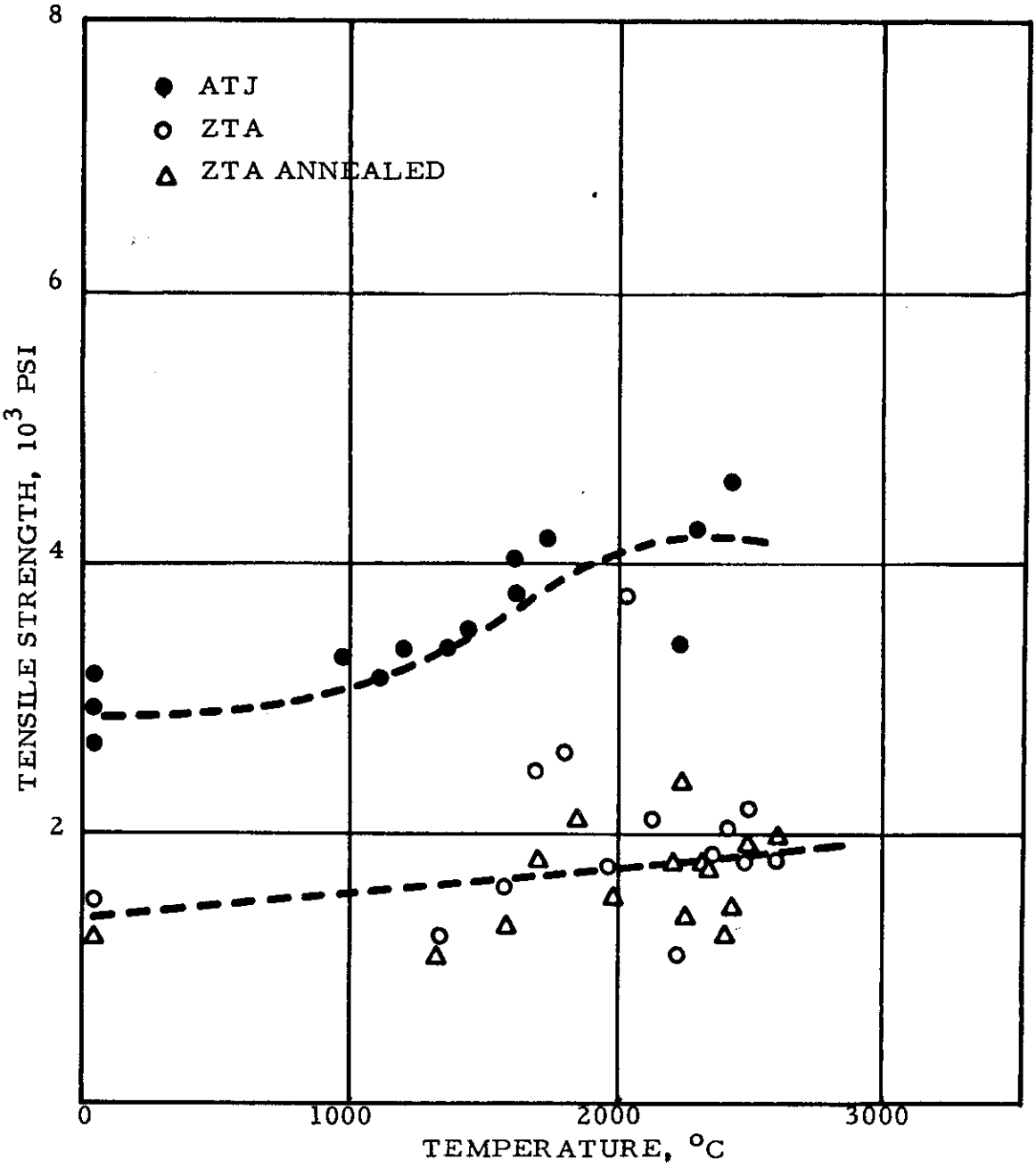

Figure 18. Short-time Tensile Strength vs Temperature - ZTA and ATJ Graphite - Across Grain.

The ultimate tensile strength of ZTA graphite is rate dependent. As is to be expected in the case of brittle materials, the higher the load rate the lower the measured tensile strength. A similar behavior (which is the inverse of the rate dependence usually exhibited by metals) was also noted in measurements of the shear strength of a polycrystalline molded graphite stock.[9] Tables 16 and 17 and Figures 19 and 20 show the effect of load rate on the strength of ZTA at temperatures of 1525°C , 1820°C, and 2235°C. It appears that the normal load rate of 0.020 inch/min. yields about the same strength as does the reduced rate of 0.002 inch/min. The notable change occurs when the rate is increased to 0.200 inch/min. Here a large reduction is consistently observed independent of state of anneal or orientation, particularly at the higher temperature.

Table 16. Temperature-Strength Data for ZTA Graphite Oriented With Grain Variable Load Rate

Specimen No.	Load Rate in/min.	Temperature °C (°F)	Ultimate Tensile Strength psi
5-14	0.002	1520 (2770)	3020
5-25	0.002	1525 (2775)	2835
5-28	0.002	1525 (2775)	3215
5- 1	0.020	1525 (2775)	3120
5-11	0.020	1525 (2775)	2835
5-15	0.020	1525 (2775)	2985
5- 8	0.200	1525 (2775)	3405
5-21	0.200	1530 (2785)	2960
5-24	0.200	1525 (2775)	2780
5- 2	0.002	1825 (3315)	4610
5-13	0.002	1830 (3325)	4490
5-23	0.002	1830 (3325)	4260
5- 4	0.020	1825 (3315)	4390
5-16	0.020	1825 (3315)	4230
5-29	0.020	1820 (3310)	3980
5-10	0.200	1820 (3310)	4100
5-18	0.200	1830 (3325)	3930
5-22	0.200	1825 (3315)	3660
5-17	0.002	2240 (4065)	7390
5-19	0.002	2240 (4065)	6870
5-26	0.002	2240 (4065)	6380
5- 3	0.020	2235 (4055)	6840
5- 5	0.020	2240 (4065)	6530
5-20	0.020	2240 (4065)	6680
5- 7	0.200	2235 (4055)	5190
5-12	0.200	2230 (4045)	5030
5-30	0.200	2235 (4055)	4780

Table 17. Temperature-Strength Data for ZTA Graphite Oriented Across Grain Variable Load Rate

Specimen No.	Load Rate in/min.	Temperature °C	Temperature (°F)	Ultimate Tensile Strength psi
6- 1	0.002	1525	(2775)	1115
6-27	0.002	1525	(2775)	1325
6-30	0.002	1530	(2785)	1205
6- 2	0.020	1530	(2785)	1180
6- 7	0.020	1525	(2775)	1205
6-19	0.020	1520	(2770)	1365
6-16	0.200	1525	(2775)	1205
6-17	0.200	1525	(2775)	1365
6-28	0.200	1525	(2775)	1460
6-10	0.002	1820	(3310)	1870
6-12	0.002	1825	(3315)	1660
6-26	0.002	1830	(3325)	1660
6-11	0.020	1820	(3310)	1840
6-21	0.020	1825	(3315)	1640
6-29	0.020	1825	(3315)	1960
6- 8	0.200	1825	(3315)	1520
6-13	0.200	1825	(3315)	1650
6-18	0.200	1830	(3325)	1560
6- 5	0.002	2240	(4065)	2250
6-14	0.002	2240	(4065)	2380
6-15	0.002	2240	(4065)	1910
6- 4	0.020	2240	(4065)	2100
6-24	0.020	2235	(4055)	2000
6-25	0.020	2235	(4055)	1880
6- 6	0.200	2235	(4055)	1720
6- 9	0.200	2235	(4055)	1590
6-22	0.200	2235	(4055)	1650

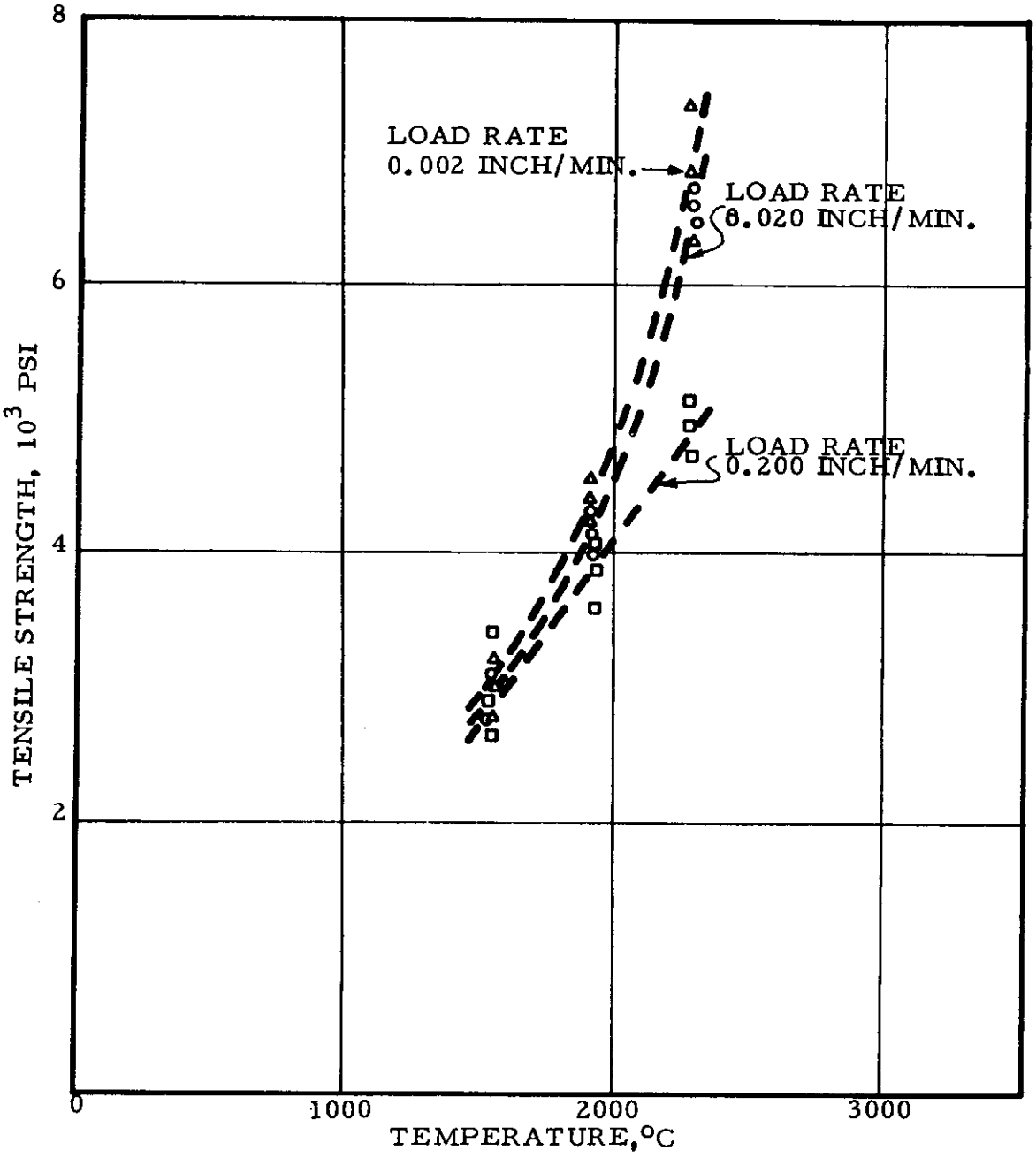

Figure 19. Short-time Tensile Strength vs Temperature - ZTA Graphite With Grain - Variable Load Rate.

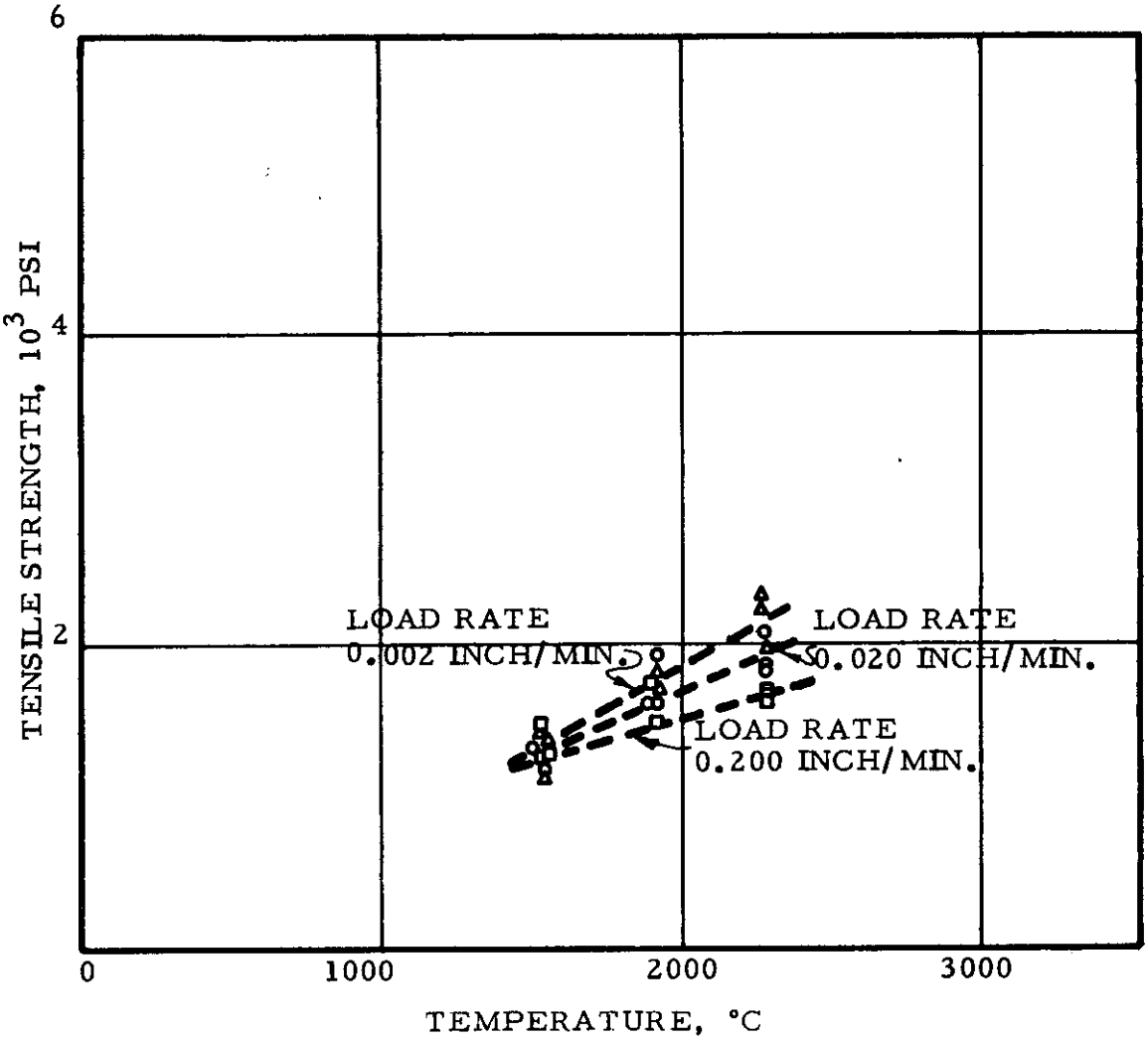

Figure 20. Short-time Tensile Strength vs Temperature - ZTA Graphite Across Grain - Variable Load Rate.

3.2.4 Electron Microscope Studies of the Fracture Surfaces of ZTA Graphite

Electron microscope replicas of the fracture surfaces obtained at elevated temperatures have been taken in the Aeronutronic Subcontract for specimens representing the different groups tested. It should be recognized that some of the fine details of these micrographs may reflect variations encountered in the replicating process and may not be truly representative of the fracture surfaces. Typical surfaces are shown in Figures 21-24 for the cross grain orientations of the ZTA graphite. Figures 25-28 represent typical surfaces when the specimens were oriented with the grain.

The breaks that have been observed to date can be classed in two general categories:

(a) Moderately smooth and oriented near normal to the stress axis;
(b) Very rough and irregular and oriented 60° to 70° from the stress axis.

The first category is typical of the fracture surface obtained by the ZTA graphite broken in the cross grain direction independent of the state of anneal. The breaks seem to be principally grain boundary separation with little, if any, grain fracture. Where grain fracture appears to occur, the surface resembles that observed on delamination of a pyrolytic material.

The latter category is typical of the fracture surface of the ZTA graphite when oriented with the grain. Here one observes areas wherein the break seems to be in the grain as indicated by the layered fracture (see Figure 26 (b)). Normally, the areas adjacent to this layered type breaking show regions of extreme irregularity as noted in Figure 26 (a). What appears to be happening is a general grain fracture that propagates to a particle boundary. At the boundary, the fracture surface moves up or down to seek the following surface of least resistance. The trend of motion between grain fracture surfaces seems to be grossly in one preferred direction. This preferred direction might be partially explained by the conchoidal nature of many of the fractures. Unfortunately, the lower magnifications of the electron microscope tend to lose the detail needed to identify the conchoidal nature, while the magnification that was used limits the field of vision to the extent that one cannot photograph the region of interest.

One interesting nature of the fracture that does not lend itself to electron microscopy is the occurrence of spires on the fracture surface (the other surface shows a corresponding hole). These spires vary in size up to about 0.05 inch on a side and 0.05 inch high and are generally rectangular in cross section. The vertical orientation is always parallel to the maximum stress direction. This system of breaking resembles the local laminar sheet noted on pyrolytic graphite failures.

3.2.5 Permeability of ZTA Graphite

One physical property of graphite which has received considerable emphasis and study recently is permeability to gases. Flow through granular media and consolidated material of relatively high permeability, such as standard commercial graphite, generally follows Darcy's law and is well understood. However, with the pore size of ZTA graphite, Darcy's law does not hold since diffusive as well as

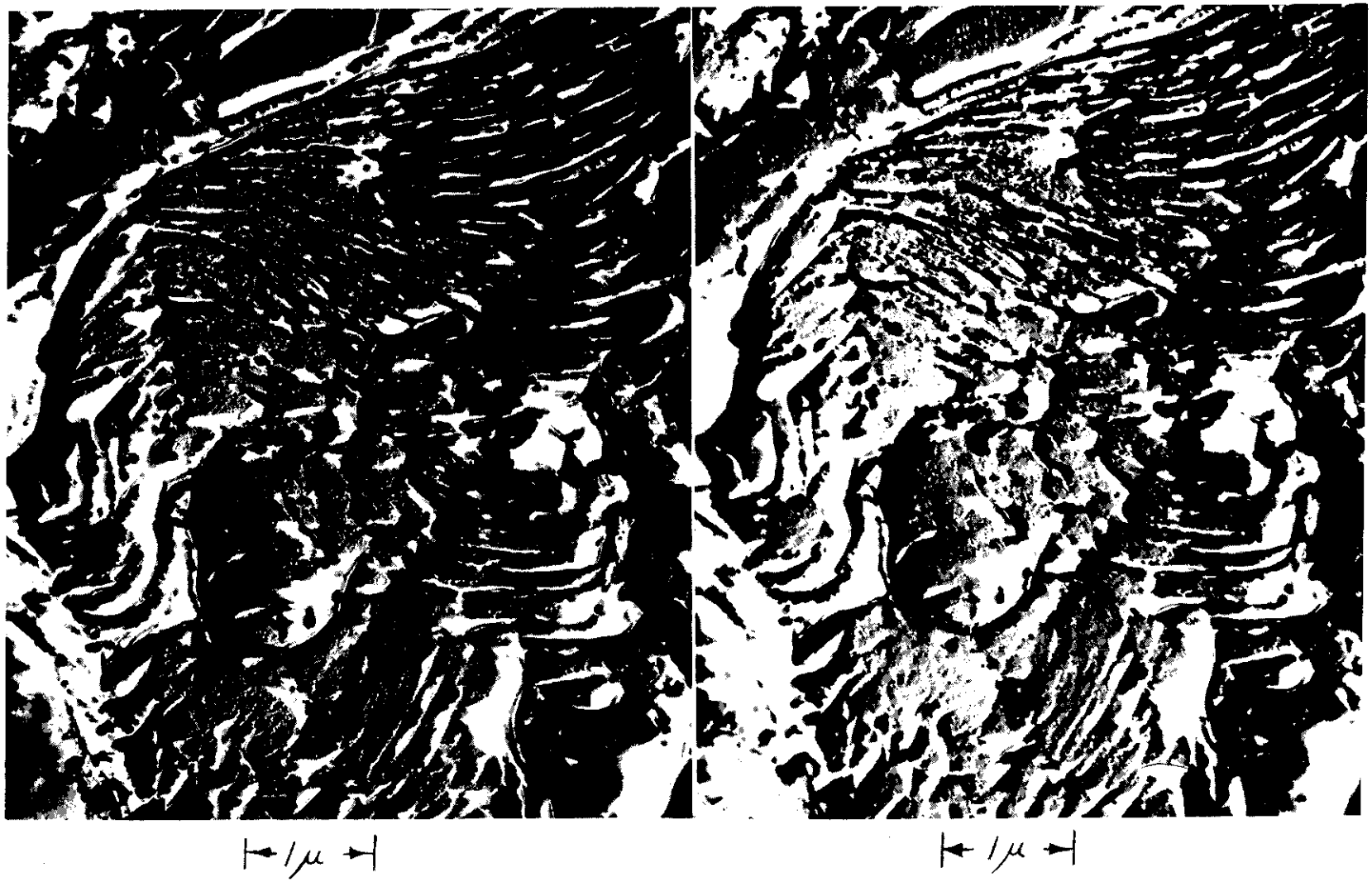

N-2495 N-2496

(a) (b)

Figure 21. Fracture Surface - ZTA Specimen 3-13, 3000°C Annealed and Oriented Across Grain. Stereo Pair of Break at 2565°C.

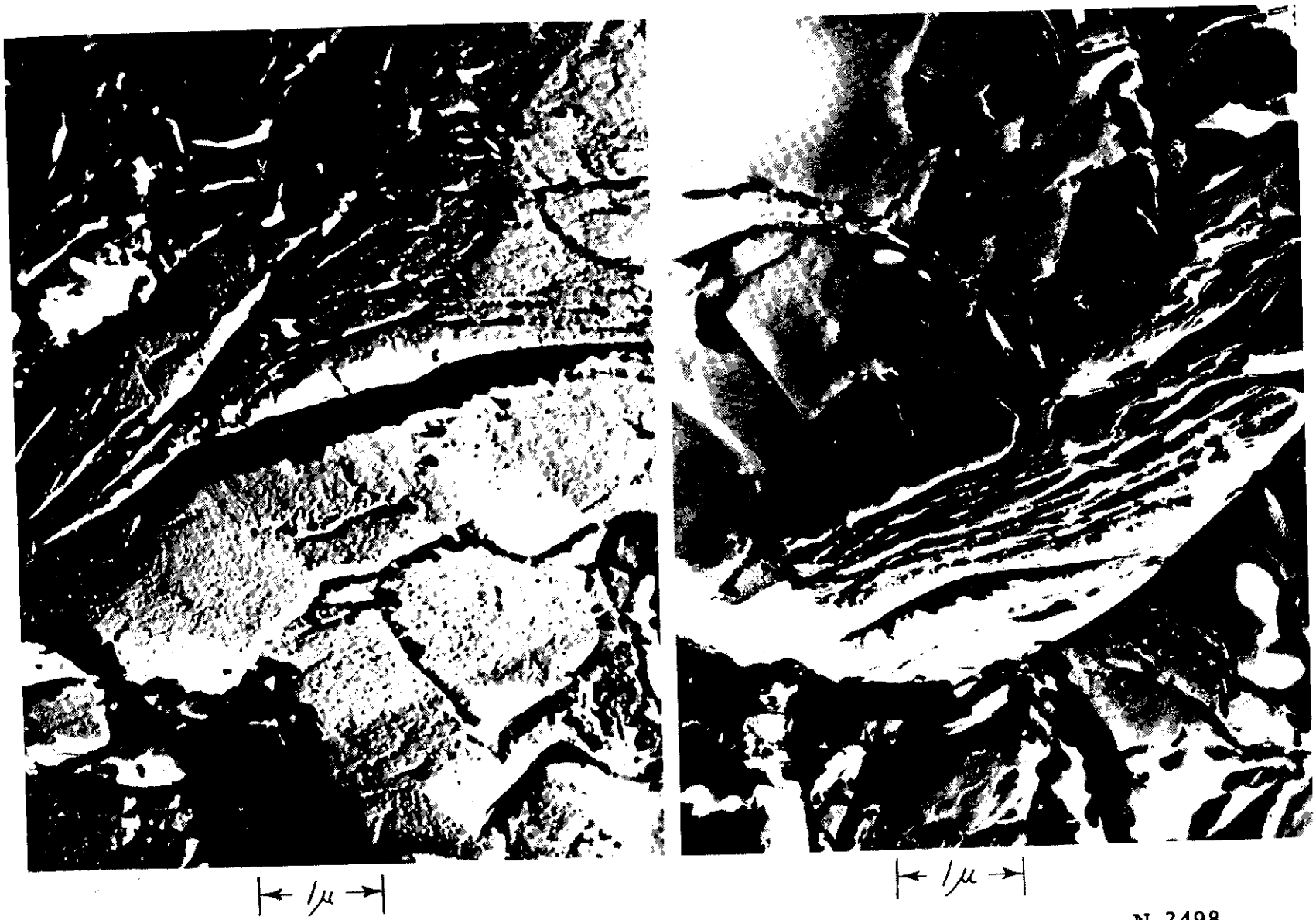

Figure 22. Fracture Surfaces - ZTA Graphite Specimen 3-13, 3000°C. Annealed and Oriented Across Grain. Broken at 2565°C.

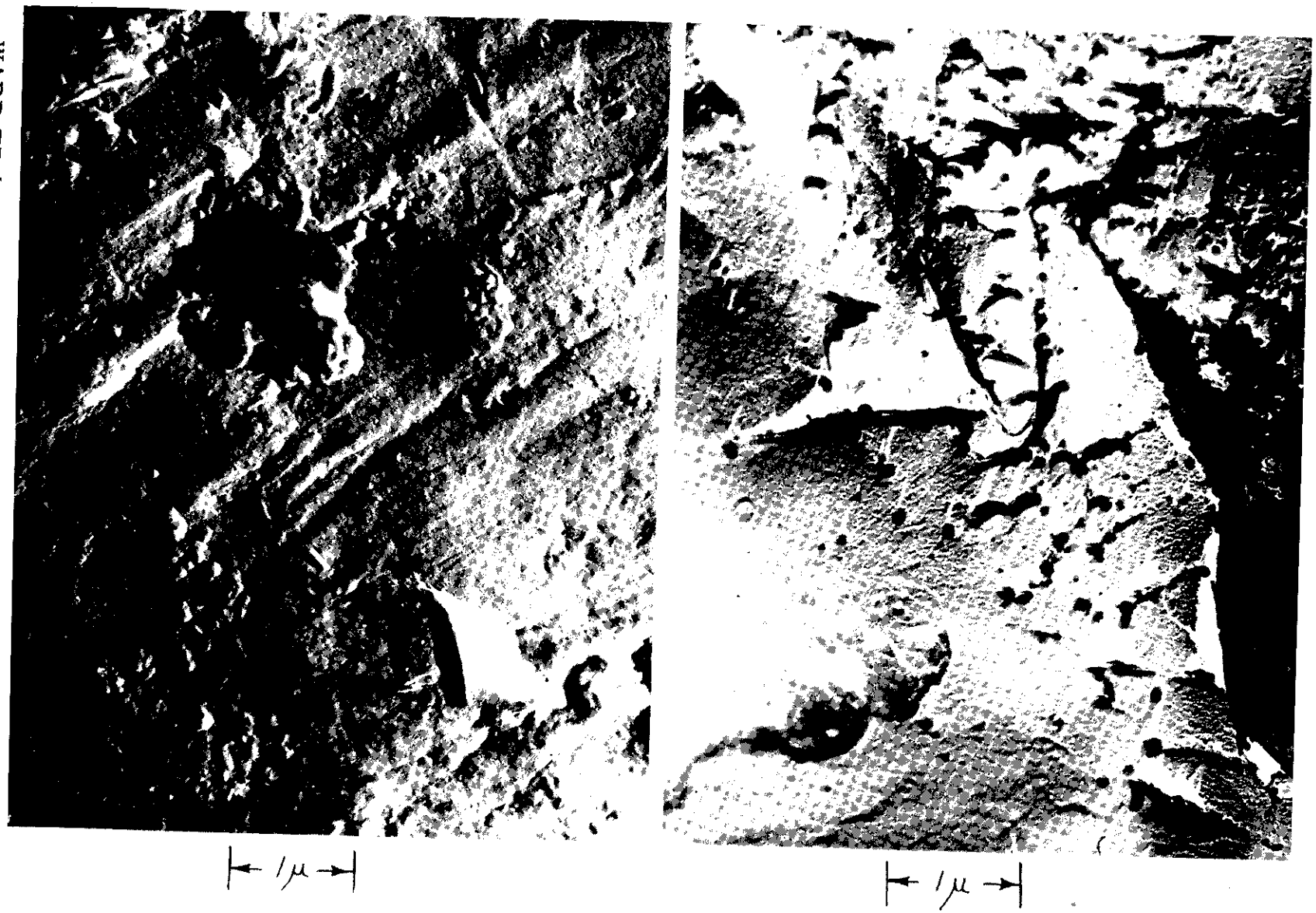

(a) (b)

Figure 23. Fracture Surfaces - (a) ZTA Graphite Specimen 3-13, 3000°C. Annealed and Oriented Across Grain, Broken at 2565°C, (b) ZTA Graphite Specimen 1-20, Oriented Across Grain, Broken at 2455°C.

Figure 24. Fracture Surfaces - ZTA Graphite Specimen 1-20, Oriented Across Grain, Broken at 2455°C.

Figure 25. Fracture Surface - ZTA Graphite Specimen 4-15, 3000°C Annealed and Oriented With Grain. Stereo Pair of Break at 2610°C.

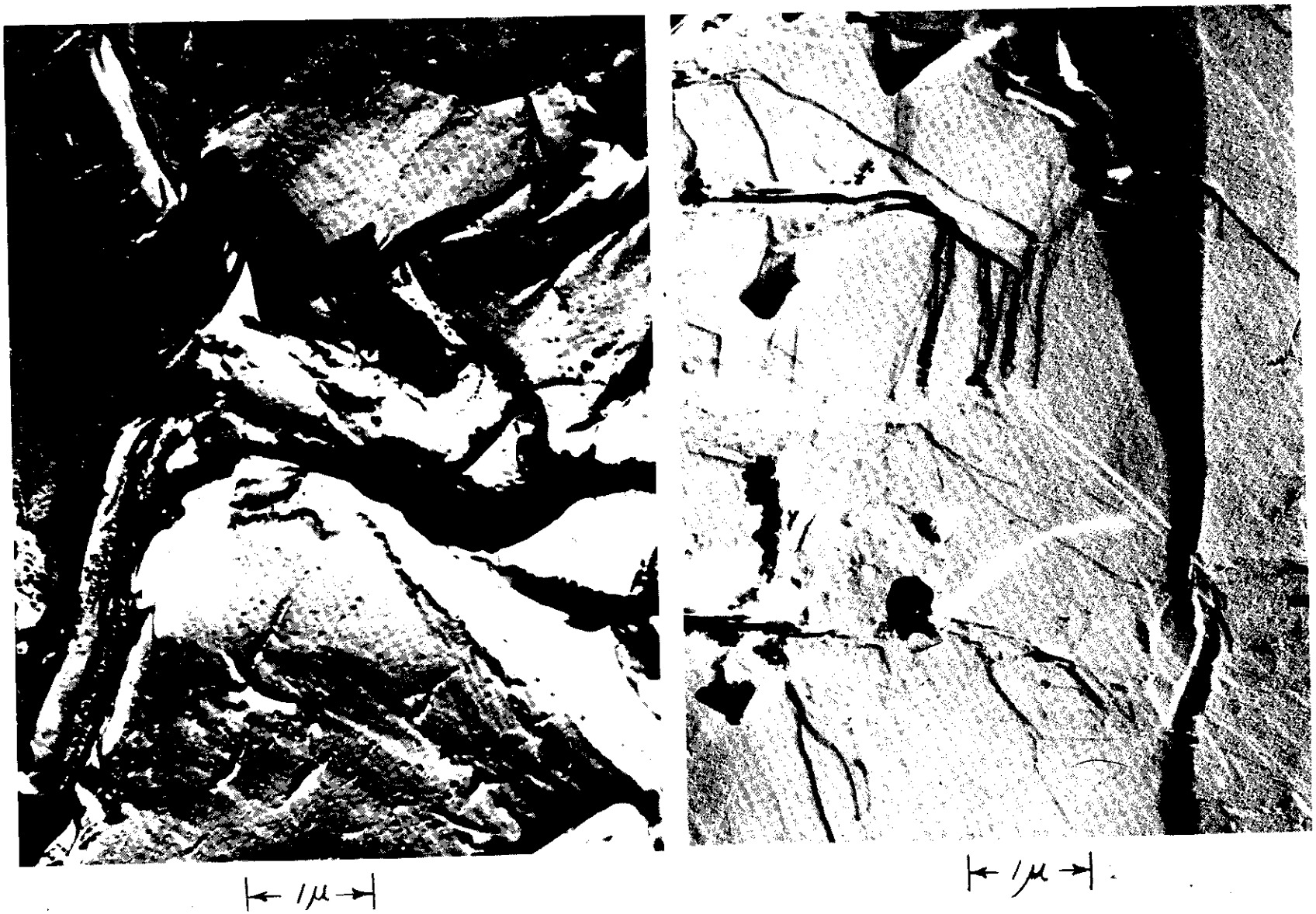

Figure 26. Fracture Surfaces - ZTA Graphite Specimen 4-15, 3000°C. Annealed and Oriented With Grain, Broken at 2610°C.

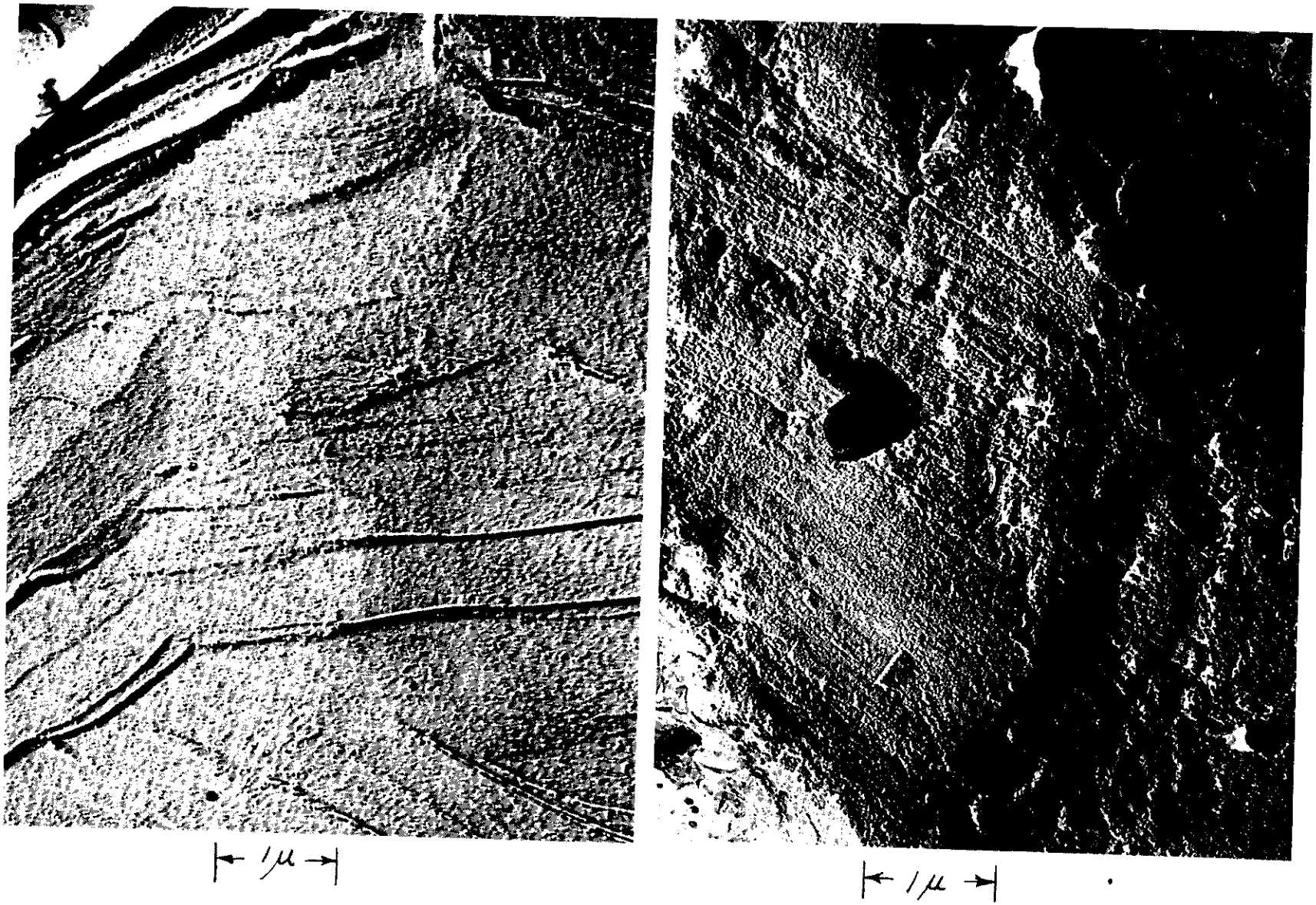

Figure 27. Fracture Surfaces - (a) ZTA Graphite Specimen 4-15, 3000°C Annealed and Oriented With Grain, Broken at 2610°C, (b) ZTA Graphite Specimen 2-21, Oriented With Grain, Broken at 2455°C.

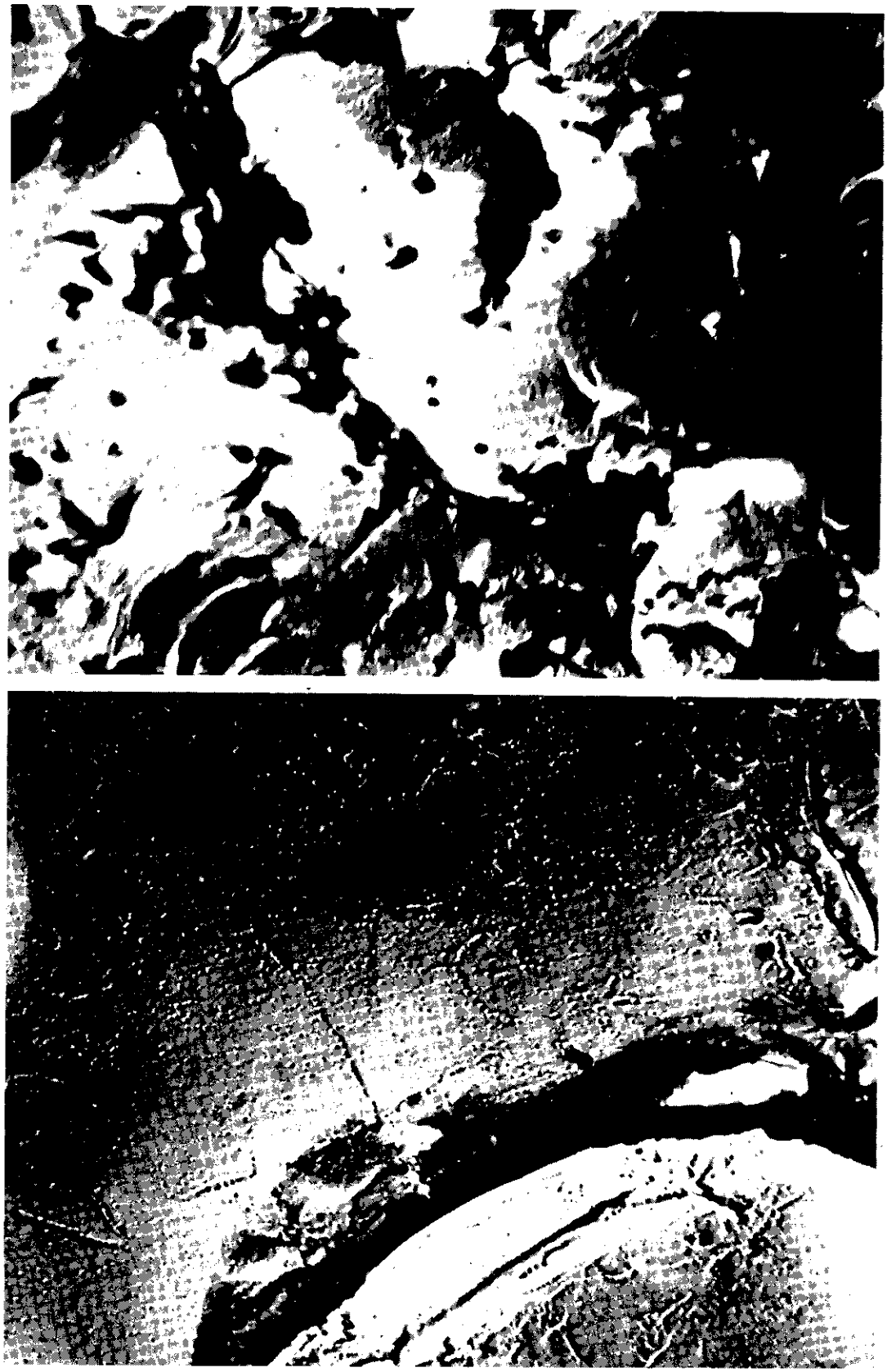

N-2509 (a) N-2510 (b)

Figure 28. Fracture Surfaces - ZTA Graphite Specimen 2-21, Oriented With Grain, Broken at 2455°C.

viscous flow comes into play. The permeability of this material can be characterized by two coefficients, one for viscous flow and one for diffusive flow, according to the following formula:

$$Q_{pv} = (F_0 + F_1 \bar{p})(\frac{A}{L} \Delta p)$$

where

Q_{pv} = Pressure volume flow in milliliter - atmosphere/second

F_0 = Diffusive flow factor = $K_0\sqrt{\frac{T}{M}} = K_0^1\sqrt{\frac{T}{M}}\left(\overline{\frac{Nr^3}{X}}\right)$

F_1 = Viscous flow factor = $\frac{K_1}{\eta} = \frac{K_1^1}{\eta}\left(\overline{\frac{Nr^4}{X}}\right)$

$\bar{p}$ = Average pressure, atmospheres

A = Sample area, cm^2

L = Sample length, cm

Δp = Pressure differential across sample, atmospheres

The diffusive and viscous flow factors are related by the above equations to the properties of the gas and to the pore characteristics of the solid as defined below:

T = Absolute temperature, °Kelvin

M = Molecular weight of gas

η = Viscosity of gas, poise

N = Effective number of pores/cm^2

r = Effective pore radius, cm

X = Tortuosity factor for non-straight pores

K_0, K_1, K_0^1, K_1^1 = Constants

The permeability to helium has been determined for grade ZTA both in directions with and across the grain. The permeability coefficients, F_0 and F_1, for both ZTA and ATJ for comparison are given in Table 18. The degree of anisotropy of ATJ is such that the with the grain and across the grain permeabilities are approximately the same, hence, only the average of the two directions is given. Note that the value of F_0 for ATJ is not detectable nor is a value of F_1 for ZTA.

Table 18. Permeability to Helium of ZTA and ATJ Graphite

Grade	Sample Orientation	Permeability Coefficients F_0 (cm²/sec.)	F_1 (cm²/sec.-atm.)
ZTA	With the grain	2.1×10^{-5}	0
ZTA	Across the grain	2.5×10^{-5}	0
ATJ	Both directions	-----	0.3

The pore size of ATJ is such that the flow of gases through it follows Darcy's law, i.e., all viscous flow. The permeability of ATJ is therefore adequately described by

$$Q_{pv} = F_1 \bar{p} \frac{A}{L} \Delta p$$

The pore size of ZTA, on the other hand, is such that the viscous flow factor, F_1, effectively vanishes and the permeability can be fully described by

$$Q_{pv} = F_0 \frac{A}{L} \Delta p$$

The significance of this is that the flow of gases through ZTA is non-pressure sensitive, i.e., the ratio $Q_{pv}/\Delta p$ remains constant regardless of the magnitude of $\bar{p}$.

Although the recent emphasis on low permeability graphite has been primarily in the field of nuclear reactors and chemical process equipment, there is growing evidence that this property greatly influences the performance of graphite materials as rocket nozzles and other missile components. The low permeability and small pore size (90% less than 0.5 micron diameter) of ZTA graphite minimize the penetration of gaseous reaction products into the nozzle; the reduced penetration having been shown conclusively by the radiographic examination of fired MERM nozzles.[10]

3.2.6 Thermal and Electrical Properties of ZTA Graphite

The effect of anisotropy is most pronounced in the thermal properties of graphite, and thermal expansion is the most common parameter used to define the degree of anisotropy. Because of this and the fact that thermal porperties are of extreme importance under conditions which require graphite as a structural material, two properties - - thermal expansion and thermal conductivity -- have been determined on fairly large numbers of ZTA samples. The average room temperature values for both ZTA and ATJ graphites are given for comparison in Table 19. Insufficient data are available on these properties to permit the calculation of a standard deviation; however, the values presented here are quite typical. The anisotropy of ZTA graphite mentioned above is evident in the thermal expansion values with the across grain to with grain ratio being 13.9 as compared to 1.48 for the more isotropic ATJ. Thermal conductivity of ZTA shows an increase of 30 per cent along the grain over ATJ, but a decrease of 10 per cent across the grain, indicating more preferred crystal orientation in the ZTA.

Table 19. Average Room Temperature Thermal and Electrical Properties of ZTA and ATJ Graphites

Property	Units	With Grain		Across Grain	
		ZTA	ATJ	ZTA	ATJ
Coefficient of Thermal Expansion (Average 20-100°C)	10^{-7} °C^{-1}	6.15	23.4	85.2	34.6
Thermal Conductivity	$\frac{\text{BTU-ft.}}{\text{hr. ft}^2\ \text{°F}}$	84.0	64.5	48.0	52.5
Specific Resistance	μ ohm-cm	691	1160	2300	1430

In addition to the room temperature values, the coefficients of thermal expansion of ZTA and other graphites have been determined at temperatrues to 2500°C. Figure 29 shows the average thermal expansion coefficient from room temperature to 1000°C, both with and across the grain, plotted as a function of bulk density. The expansion coefficient increases smoothly with increasing density for the direction across the grain, reaching its highest value with single crystal graphite. Opposite behavior is shown for expansion along the grain. Figures 30 and 31 show the differential thermal expansion respectively with and across the grain for temperatures ranging from room temperature to 2500°C. Note that the expansion coefficient of ZTA approaches that of pyrolytic graphite with the grain but not across the grain.

3.2.7 Specifications for ZTA Graphite

The following property specifications have been established for grade ZTA:

1. Integrity of Structure. Grade ZTA is certified to be free of internal cracks, voids, or other structure imperfections as detectable by normal radiographic inspection techniques.

2. Bulk Density. 1.92-1.97 gm/cm^3 as measured on full size pieces.

3. Ash. Less than 0.25 per cent.

4. Pore Size. No pore larger than one micron, 90 per cent of pores smaller than 0.5 micron diameter as determined by mercury porosimetry.

5. Permeability (Helium). Less than 5×10^{-3} cm^2/sec. (F_0).

6. Anisotropy. Greater than three based on ratio of across grain to with grain thermal expansion coefficients (Average 20° to 100°C).

7. Modulus of Rupture. 5000 psi average with the grain, 2500 psi average across the grain.

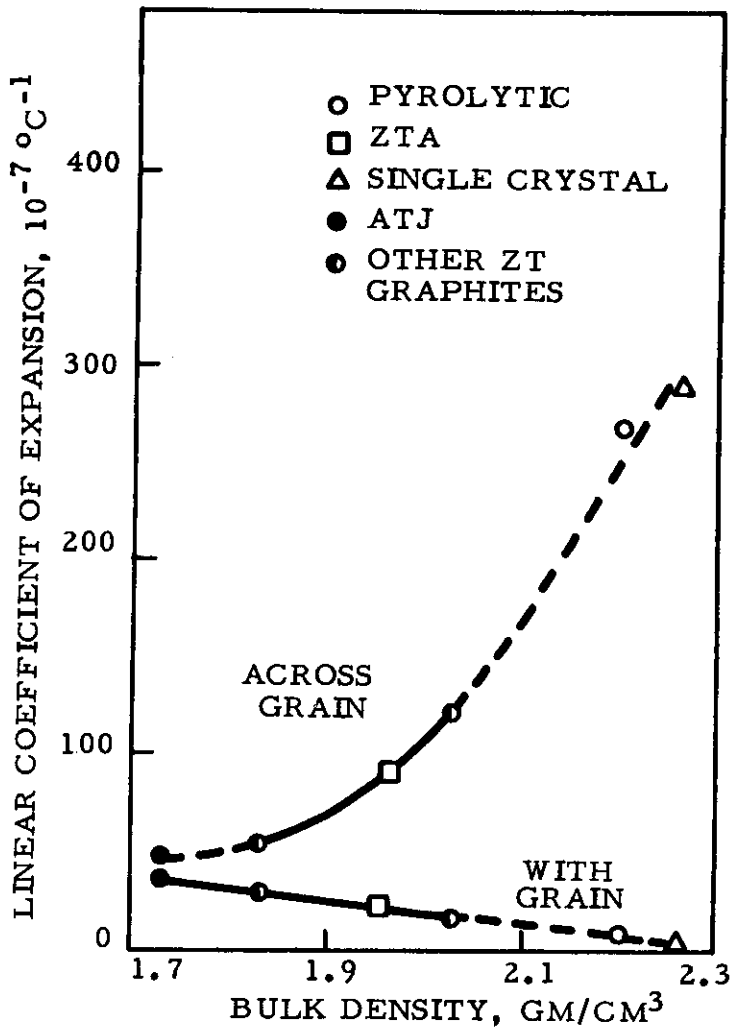

Figure 29. Thermal Expansion of Various Graphites vs Bulk Density, Average Room Temperature - 1000°C.

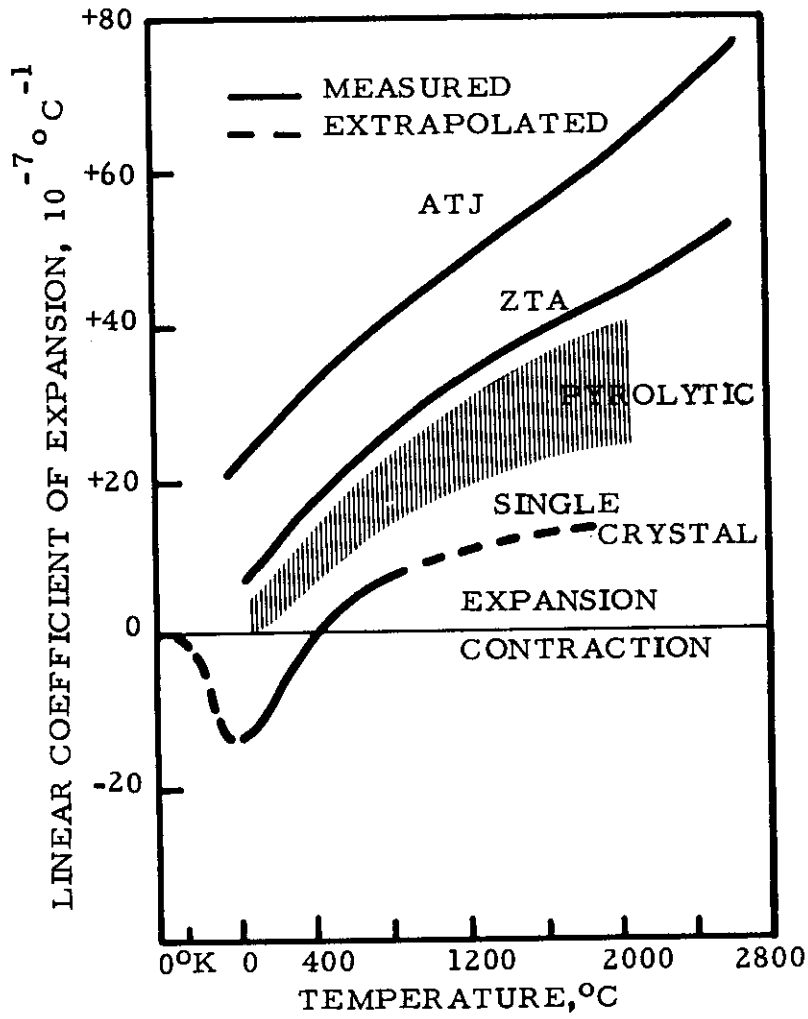

Figure 30. Thermal Expansion of Various Graphites vs Temperature (With Grain).

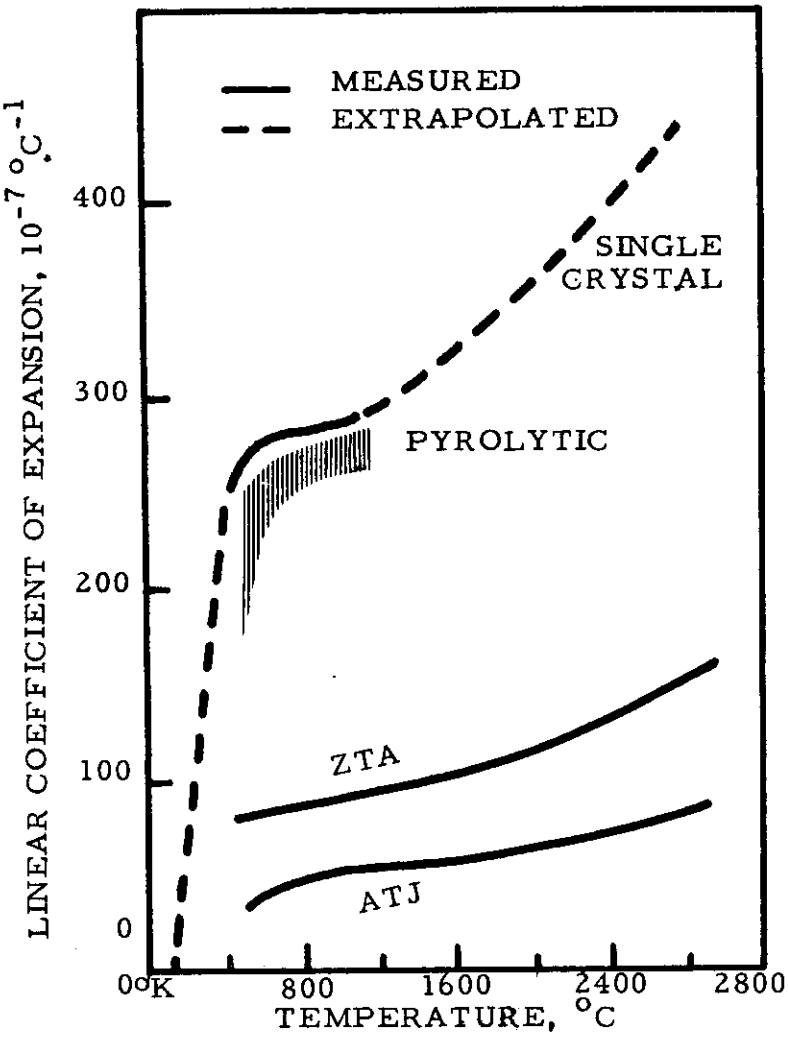

Figure 31. Thermal Expansion of Various Graphites vs Temperature (Across Grain).

3.3 Thermal Shock Resistant ZT Graphite

The resistance of graphite to thermal shock is one of the key properties which has made it indispensable for certain high temperature applications; however, as manufactured commerical graphites increase in bulk density and anisotropy, their susceptibility to thermal failure generally increases.

The very highly oriented graphites - pyrolytic and single crystal - are even more subject to thermal failure than the finest grain standard graphites. Because of the high degree of preferred grain orientation in pyrolytic graphite, it possesses superior thermal and mechanical properties in only one direction, ie., along the grain. Across the grain properties such as low strength, low thermal conductivity, and very high thermal expansion coefficients, in combination with structural imperfections, result in frequent failures - delaminations - when the pyrolytic material is subjected to thermal and mechanical stresses.

In the manufacture of graphite electrodes, it is well established that finer grain graphites are not as resistant to thermal failure as electrodes which contain coarser particles. As discussed in Section 1, some electrodes contain particles as large as 0.5 inch diameter, whereas the fine grain specialty graphites rarely contain particles larger than 0.03 inch diameter. Graphite electrodes containing larger particles are more isotropic in properties than the fine grain graphites and this accounts in some degree for their greater resistance to thermal shock; however, the greater thermal shock resistance is accompanied by a sacrifice in other property values such as higher porosity, lower strength, etc.

The high density ZT graphites, such as the ZT-X001 series, are not different from pyrolytic or standard fine grain graphites in this respect, ie., they too are subject to thermal failure. The tendency toward failure is proportional to bulk density and, hence to other factors such as anisotropy. To alleviate this deficiency in an otherwise superior graphite, a new series of high density (ZT) graphites was developed. This series is essentially a modification of the ZT-X001 series, the modification being the use of a starting material possessing excellent thermal properties and a larger particle size. The grain size of this material is similar to that found in small graphite electrodes employed in electric furnaces. This new "hot worked" graphite has been given the experimental designation ZT-X007 and it is processed, with minor modifications, in the same manner as the ZT-X001 graphites. Figures 32-35 show the structure of a typical member of this series (ZT-5007) at 20X and 75X before and after processing. Typical physical properties of ZT-5007 compared to its counterpart, ZT-5001, are given in Table 20.

Although not as mechanically strong or impervious as ZT-5001, the ZT-5007 graphite should be more resistant to thermal failure, especially because of its high thermal conductivity. ZT-5007 is somewhat remarkable in this respect - the across-the-grain value is better than the best with-the-grain conductivities of standard commercial graphites. The with-the-grain value for ZT-5007 approaches that of pyrolytic graphite. Permeabilities, although higher than those of ZT-5001, are still lower (by factors of the order of 100 to 1000) than the lowest permeability normally fabricated graphites. Also worthy of note is the lower across-the-grain electrical resistivity of ZT-5007 compared to ZT-5001.

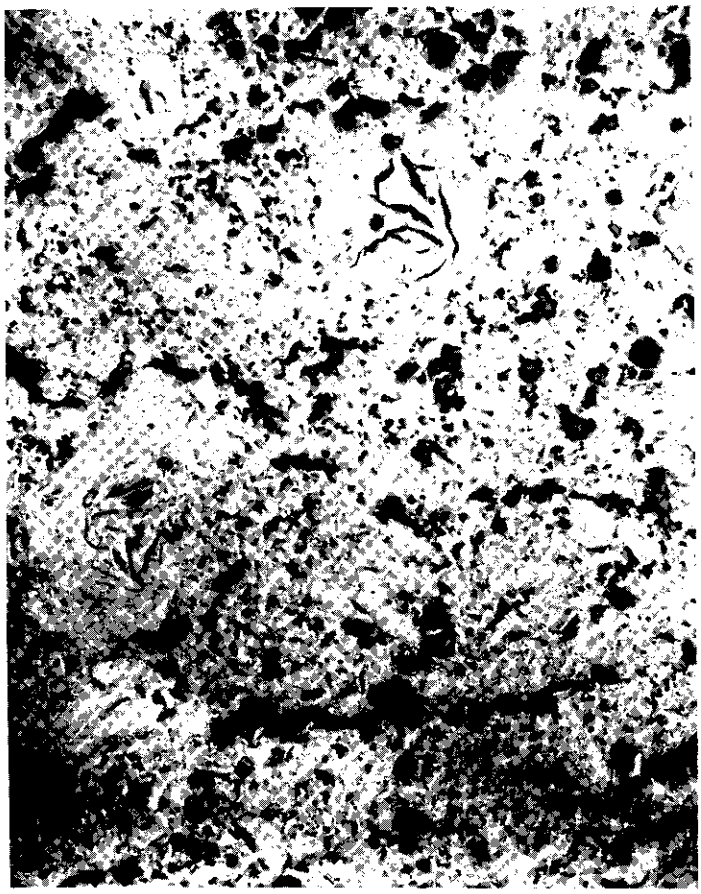

Figure 32. Photomicrograph of ZT-5007 Before Processing, Magnification 20X.

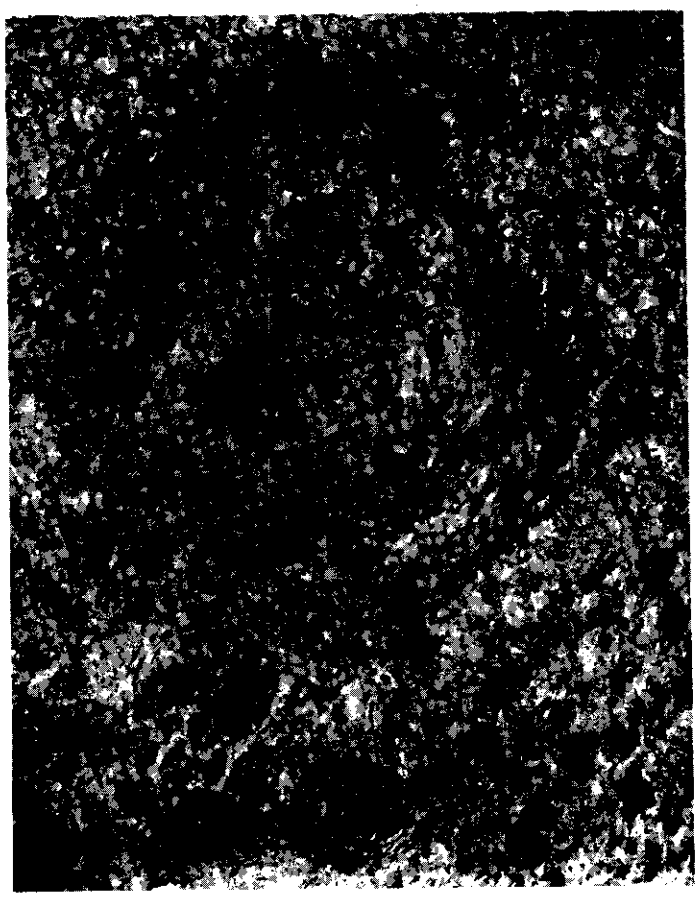

Figure 33. Photomicrograph of ZT-5007 After Processing, Magnification 20X.

Figure 34. Photomicrograph of ZT-5007 Before Processing, Magnification 75X.

Figure 35. Photomicrograph of ZT-5007 After Processing, Magnification 75X.

Table 20. Room Temperature Physical Properties of ZT-5007 and ZT-5001 Graphites

Property	Units	With Grain		Across Grain	
		ZT-5007	ZT-5001	ZT-5007	ZT-5001
Bulk Density	gm/cm^3	2.00	2.00	2.00	2.00
Specific Resistance	μ ohm-cm	580	650	770	2000
Modulus of Rupture	psi	2600	7000	1700	2300
Young's Modulus	10^6 psi	1.64	3.00	0.80	0.70
Coefficient of Thermal Expansion	$10^{-7} °C^{-1}$	12	4	75	95
Thermal Conductivity	$\frac{BTU\text{-}ft}{hr.ft^2 °F}$	154	85	93	45
Permeability (He)	F_0, $cm^2/sec.$	7×10^{-3}	2×10^{-5}	7×10^{-4}	2.5×10^{-5}
	F_1, $cm^2/sec\text{-}atm$	2×10^{-3}	0	1.5×10^{-3}	0

Using the parameter KS/αE* as an indication of the relative thermal shock resistance, ZT-5007 has a value almost double that of ZT-5001 using across the grain properties in both cases. The higher the value of this parameter, the greater the resistance to thermal shock.

The physical properties of ZT-X007 as a function of bulk density have not as yet been studied as extensively as those of ZT-X001 graphites (see section 3.1); however, the effect of density on one property, coefficient of thermal expansion, is worthy of note here. Figure 36 shows the relation between thermal expansion and bulk density for two varieties of ZT graphites. The notable features of this relationship are the identical slopes for the widely different materials, ZT-X007 vs ZT-X001.

3.4. Physical Properties of Miscellaneous ZT Graphites

The two series of ZT graphites discussed above represent only a very small segment of the varieties produced in the laboratory so far and have only scratched the surface of possibilities. The field of ZT composites of graphite and inorganic compounds is just beginning to be explored and will not be discussed here. The discussions in the preceding sections and that which follows are limited to all-graphite materials. No attempt will be made to fully cover all ZT graphites under development; however, several experimental grades are worthy of limited discussion. The first of these is the ZT-X501 series and its modifications (ZT-X502 through ZT-X508) which are processed directly from powdered materials.

*K = thermal conductivity
S = tensile strength
α = coefficient of thermal expansion
E = modulus of elasticity

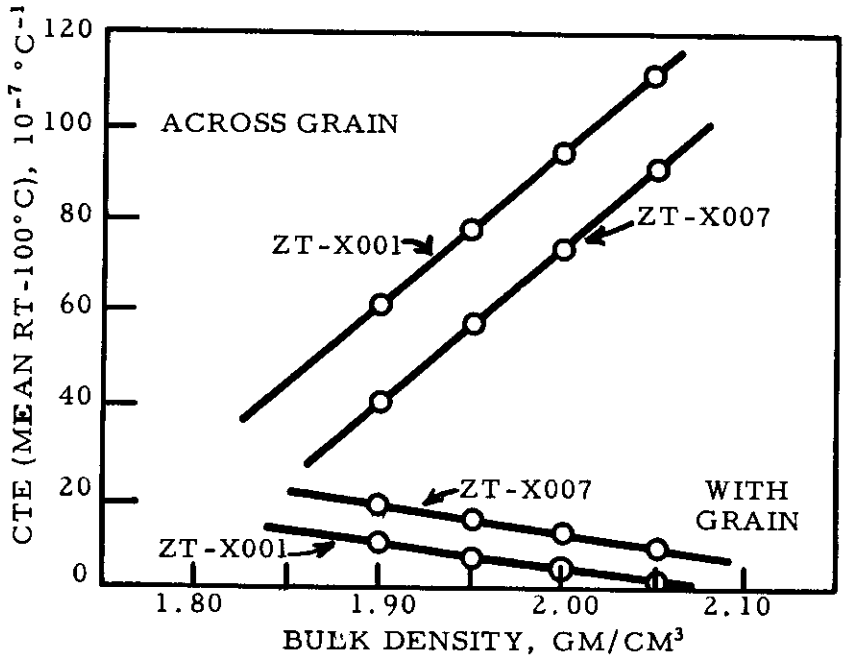

Figure 36. Linear Coefficient of Thermal Expansion of ZT Graphite, Average from Room Temperature to 100°C

The spectra of physical properties of these types of ZT graphite cover wider ranges than those of either of the grades discussed in sections 3.1, 3.2, and 3.3. For example, the ZT-X507 series showed anisotropy ratios based on thermal expansion coefficients ranging from 6 to 100 to extremes where contraction along the grain occurred in the 20-100°C range not unlike single crystal behavior. In general, bulk densities of these grades are above 2.00 gm/cm^3, and some specimens approach 2.20 gm/cm^3. As expected, these grades are not as resistant to thermal shock as the ZT-X007 graphites; however, certain properties such as the high thermal conductivities and low thermal expansions along the grain make these materials extremely interesting. Physical properties of a representative member of this type of ZT graphite, ZT-7501, are given in Table 21.

The ZT-X501 and associated grades are at the present time limited in size to approximately 5" diameter by 5" long with available equipment. ZTA is also at the present time limited to a maximum size of approximately 14" diameter by 10" long. The need for larger sizes of ZTA and other ZT graphites is recognized, however this work has not progressed to the point where larger size ZTA has yet been produced. Experiments with alternate starting materials have resulted in the establishment of a new grade, ZTE, which will eventually be available in sizes up to 30" diameter. This grade employs as its starting material a large diameter specialty graphite which contains a slightly larger particle size than that found in ZTA; however, the uniformity of this starting material is superior to the starting material for ZTA and it is anticipated that this uniformity will be reflected in the final ZTE properties. Only limited physical property data are available on this material; however, at a bulk density level of 1.95 to 2.00 gm/cm^3, these properties fall between those of ZTA and ZT-5007. Improvements in equipment

Table 21. Physical Properties of ZT-7501 Graphite

Property	Units	With Grain		Across Grain
Bulk Density	gm/cm^3		2.129	
Specific Resistance	μ ohm - cm	390		1902
Young's Modulus	10^6 psi	2.20		.51
Modulus of Rupture	psi	4025		1415
Coefficient of Thermal Expansion (Average 20°-100°C)	10^{-7} °C^{-1}	4.85		110.5
Thermal Conductivity*	$\frac{BTU\text{-}ft.}{hr.\ ft.^2\ °F}$	205		42
Ash	%		0.026	

* Calculated under the assumption that the product of Thermal Conductivity and resistivity equals 33×10^{-5} ohm cal sec^{-1} $°K^{-1}$.

and processing techniques should result in an improvement in these properties as was accomplished during the course of ZTA development.

4. PERFORMANCE TESTING OF ZT GRAPHITES

During the course of ZT graphite development, a considerable number of sub-scale firings of the experimental materials were conducted in solid fuel test motors at various locations. Agencies and contractors participating in this testing were Aerojet-General, Atlantic Research, Battelle Memorial Institute, Bendix Products, Hercules Powder, NASA, Picatinny Arsenal, Rohm and Haas, Thiokol, and others. No attempt will be made to discuss in detail the testing at these locations; however, it would seem appropriate to summarize the results of the firings of the ZT graphites along with those of other graphite materials to illustrate the significant advances made in graphite as a nozzle material.

Tables 22 through 24 summarize the firing results as received from the various test locations. Table 22 gives the results with 5500°F propellant flame temperature fuel, Table 23 with 6000°F + propellant flame temperature fuel, and Table 24 with miscellaneous fuels. The results have been grouped in these three categories for simplicity and no attempt has been made to differentiate between the fuels used at different locations. The data are presented here to show the marked superiority of the ZT graphites over standard commercial graphites as a nozzle material in solid propellant rocket motors.

From the data presented in Tables 22 through 24 it is possible to draw several conclusions. First, the erosion rate of ZTA is approximately one-fifth that of ATJ when fired under identical conditions with 5500°F fuel (see Table 22). When fired with a highly oxidizing 6000°F + fuel, the erosion rate is extremely pressure sensitive, ranging from 1.7 mil/sec. at 800 psi downward to 0.5 mil/sec. at 300 psi.

Table 22. Subscale Firing Data on National Carbon Graphites - 5500°F Fuel

No.		Test Location	Throat Dia Initial in.	Pressure psi	Duration sec.	Erosion Rate Mil/sec. - radius	% Ave. Change
1	ATJ	Aerojet-General	0.473	892	59	0.746	40.2
2	ATJ	"	0.485	800	60	0.658	35.0
3	ATJ	"	0.471	779	58	0.448	31.0
4	ATJ	"	0.474	1030	60	0.250	13.0
5	RT-0003	"	0.472	840	55	0.746	37.8
6	RT-0003	"	0.483	805	61	0.689	37.8
7	B-2540	"	0.460	830	59	0.967	55.2
8	B-2540	"	0.478	820	61	0.476	25.7
9	Pyrolytic on ATL	"	0.477	893	60	0.175	9.0
10	Pyrolytic on ATL	"	0.472	898	60	0.066	3.4
11	Pyrolytic on Graph. Cloth	"	0.469	852	60	0.434	20.3
12	Pyrolytic on Graph.Cloth	"	0.470	717	60	0.684	37.9
13	ZT-4001	"	0.470	1075	58	0.025	1.26
14	ZT-4001	"	0.472	985	59	0.034	1.71
15	ZT-4001	"	0.473	948	59	0.134	6.9
16	ZT-5001	"	0.475	1025	63	0.047	2.5
17	ZT-5001	"	0.476	1008	59	0.102	5.0
18	ZT-6001	"	0.5	1000	60	---	3.-
19	ZT-6001	"	0.5	1000	60	---	8.-
20	ZT-6001	"	0.5	1000	60	---	2.-
21	ZT-6001	"	0.5	1000	60	---	6.-
22	ZT-6501	"	0.5	1000	60	---	1.7
23	ATJ	Atlantic Research	0.550	1000	60+	0.9	---
24	ATJ	"	0.550	1000	60+	1.20	---
25	ZT-3001	"	0.550	1000	60+	0.30	---
26	ZT-3001	"	0.550	1000	60+	0.38	---
27	ZT-5001	"	0.550	1000	60+	0.30	---
28	ZT-6001	"	0.550	1000	60+	0.19	---
29	ZT-6001	"	0.550	1000	60+	0.27	---
30	ZT-6504	"	0.550	1000	60+	0.23	---
31	ZT-6505	"	0.550	1000	60+	0.20	---
32	ATJ	"	0.375	1900	6	3.0	---
33	ATJ	"	0.375	1900	6	3.5	---
34	ZT-4001	"	0.375	1900	6	1.0	---
35	ZT-4001	"	0.375	1900	6	1.6	---
36	ZT-4007	"	0.528	1000	30	0.60	---
37	ZT-4001	Thiokol, Huntsville	1.00	600/500	60	0.75	---
38	AGX	"	1.00	600	60	6.10	---
39	ZT-4001	Thiokol, Utah	0.875	1000	60	1.1 (Ave. of 2 tests)	

Table 23. Subscale Firing Data on National Carbon Graphites - 6000°F+ Fuel

No.	Grade	Test Location	Throat Dia. Initial in.	Pressure psi	Duration sec.	Erosion Rate Mil/sec. radius	% Ave. Change
1	ZTA	Aerojet-General	0.5551	800	90	1.7	77.
2	ZTA	"	0.620	500	78	0.9	25.
3	ZTA	"	0.733	300	90	0.85	19.
4	ZTA	"	0.726	300	99	0.3	4.4
5	ZT-3007	"	0.470	110-338	70.5	2.0	160.
6	ZT-4007	"	0.469	1065-366	65	1.6	111.
7	ZT-5006	"	0.473	945-338	55	1.3	91.
8	ZT-5001	"	0.471	980-338	68	1.4	99.
9	ZT-7501	"	0.732	364-182	86	0.46	23.
10	ZT-7501	"	0.725	289-190	85	0.46	22.7
11	ZT-5007	"	0.470	975-365	70	1.4	103.
12	ZTA	"	0.726	266-188	100	0.53	31.5
13	ZTA	"	0.510	745-325	73	1.2	78.3
14	ZTA	"	0.733	274-206	87	0.4	20.1
15	ATJ	"	0.725	282-206	92	0.56	31.3
16	ATJ	"	0.725	309-114	98	0.84	49.
17	ZT-4001	Allegany Ballistics	0.875	300	30	("one-fourth of ATJ")	
18	ZT-4001	Battelle	0.250	600	10	"none"	"none"
19	ZT-4001	Atlantic Research	0.550	1000	--	----	----
20	ZT-4007	"	0.626	1000	30	4.9	----
21	ATJ	"	0.465	1000	30	3.0	----
22	ATJ	"	0.465	1000	30	2.4	----
23	ATJ	Hercules, Utah	1.0	250	65	0.50	----
24	ZT	"	1.0	250	67	0.19	----
25	ZT-4001	Thiokol, Utah	---	700-550	51	1.2	32.
26	Pyrolytic on ZT	"	---	700-550	60	0.6	----
27	ZT-3001	Rohm and Haas	0.542	800	10	3.6	----
28	ZT-3001	"	0.542	800	10	3.5	----
29	ZT-4001	"	0.542	800	10	2.6	----
30	ZT-4001	"	0.542	800	10	3.4	----
31	ZT-5001	"	0.542	800	10	3.6	----
32	ZT-5001	"	0.542	1000	--	---	----
33	ATJ	"	0.542	800	10	5.6	----
34	ATJ	"	0.542	800	10	7.3	----

Table 24. Subscale Firing Data on National Carbon Graphites - Miscellaneous Fuels

No.	Grade	Test Location	Type Fuel	Throat Dia. Initial In.	Pressure psi	Duration sec.	Erosion Rate Mil/sec-radius
1	ATJ	Bendix Products	Linde Jet Torch	---	---	10.1	14 (0.23 gm/sec)
2	ZT-4001	Bendix Products	Linde Jet Torch	---	---	10.0	6 (0.16 gm/sec)
3	ZT-4007	Bendix Products	Linde Jet Torch	---	---	10.0	8 (0.20 gm/sec)
4	ZT-5001	Nav. Ord. Ch. Lake	Linde Jet Torch	---	---	----	None - Repeated Use
5	ZT-4001	Picatinny Arsenal	4000° Non. Al.	0.685	1000	35	0.86
6	ZT-4001	NASA, Huntsville	1KW (H_2)	0.125	---	----	None

The amounts of CO_2, H_2O, and HCl etc., in the exhaust gases, as well as the flame temperature, determine the erosion rate of graphite. Propellant chemistry, therefore, plays a decisive role in the performance of ZTA or other graphites as nozzle materials.

5. PROCESS FOR HIGH DENSITY (ZT) GRAPHITE MATERIALS

The basis of the manufacturing process for high density (ZT) graphite has been stated earlier (Section 2) i.e., carbon or graphite materials are heated to a temperature at which they become plastic and are then compressed by the application of mechanical pressure. In practice, however, the process is far from simple because few materials of construction are available which have sufficient mechanical strength to be used as tooling under the extreme temperature and pressure conditions required. The problem in transforming a laboratory curiosity into a production reality can be broken down into several parts, as follows:

A) Determination of the best means of heating the material to be pressed to high temperatures and means of transferring pressure to this material while maintaining these temperatures;

B) Selection of suitable materials of construction for molds, punches, and other components which can be used under the conditions required;

C) Protection of the components from oxidation at the temperatures in question;

D) Insulation of the material being processed to prevent excessive heat losses, and

E) Selection of proper starting materials.

The development of this process was carried out simultaneously at two locations. From this concurrent development, two different processes evolved based on previously developed proprietary processes of the National Carbon Company. At the Niagara Falls, New York, Development Laboratories the developed process was based on the use of a blend of carbonaceous materials, while at the Fostoria, Ohio, Laboratories the emphasis was on the use of prefabricated carbon and graphite starting materials.

Whereas the resulting products from both processes are identical for identical starting materials, the equipment setups and operating procedures are quite different. The Niagara Falls ZT process was initially developed on equipment capable of processing a maximum product size of 2" diameter by 2" long. Scale-up to larger sizes, which are now in production, required the acquisition of additional presses and larger power sources. This scale-up was accomplished in steps - from 2" to 5" diameter, from 5" to 8-1/2" diameter, and finally from 8-1/2" to 14" + diameter. Power requirements vary by a factor of 10 from processing 2" diameter to 14" diameter pieces; however, the size of the power source is to a larger degree dictated by the thermal efficiencies which can be obtained with the particular geometry in question. Conservation of heat by means of excessive insulation during the

heating period results in long cooling cycles. On the other hand, too little insulation results in heat losses which can approach heat input and consequently results in longer heating cycles. Therefore a compromise in the amount of insulation is used to give the best overall efficiency and shortest time cycle.

During the development of this process one of the paramount problems facing the engineers was the selection of suitable materials of construction for the various components. Items which presented the greatest problem were the mold support column (or bottom punch) and the top punches. To be satisfactory, these components had to meet the following requirements:

1) They must have a low thermal conductivity to prevent the high product temperature from reaching the external components of the equipment. High thermal conductivity would also result in excessive heat losses through the punches.

2) They must have sufficient strength to transmit the required pressure to the product at high temperatures.

Unfortunately, few materials on the market meet both requirements, particularly the latter. Here again a compromise had to be made in order to attain requirement (2). The punches and other components were fabricated from a material with a reasonably high thermal conductivity, and the required temperature gradient between the heating zone and the external components of the unit was maintained by enforced cooling of the portions outside the hot zone. This naturally resulted in a lowering of the thermal efficiency of the process; however, sufficient power was made available to compensate for these heat losses.

The ZT process which was developed at the Fostoria, Ohio, Laboratories differs from that discussed above, not only from the standpoint of starting materials, but by the method with which heating is accomplished. In general, the material of construction problems were similar; however, certain key requirements differed. This process was developed primarily on a unit capable of processing a maximum product size of 4" diameter. At the present time, scale-up to 14" diameter stock has been accomplished, incorporating considerable design change in the equipment. Power source and press capacity dictate the size which can be manufactured and the processing cycles. It should be obvious that different firing schedules and pressing conditions are required for each of the various units employed in the manufacture of ZT graphite. The type (or grade) of ZT graphite being processed influences cycles.

6. REFERENCES

1. A. M. Williamson, U. S. Patent No. 935,180.

2. C. A. Hansen, U. S. Patent No. 1,037,901.

3. S. W. Bradstreet, et al, WADC Technical Report 59-706 (1960), for example.

4. L. M. Currie, V. C. Hamister and H. G. MacPherson, "The Production and Properties of Graphite for Reactors," Proc. Int. Conf. on Peaceful Uses of Atomic Energy, Geneva, 1955, Paper PT 534.

5. H. C. Stieber and R. C. Stroup, "Measurement of Creep in Graphite at 2500°-3000°C," Paper No. 123, Electrochemical Society Meeting, September 28-October 2, 1958, Ottawa, Canada.

6. E. J. Seldin and R. N. Draper, WADD Technical Report 61-72, Volume V, "Analysis of Creep and Recovery Curves for ATJ Graphite."

7. E. J. Seldin, WADD Technical Report 61-72, Volume VI, "Creep of Carbons and Graphites in Flexure at High Temperatures."

8. G. B. Spence and W. B. Daniels, unpublished data, National Carbon Company, Research Laboratory, NCRL-18 (1960).

9. L. Green, Jr., M. L. Stehsel and C. E. Waller, "High Temperature Torsional Shear Properties of a Molded Graphite," Conference on Mechanical Properties of Engineering Ceramics, North Carolina State College, March, 1960.

10. R. W. Wallouch, WADD Technical Report 61-72, Volume IV, "Adaptation of Radiographic Principles to the Quality Control of Graphite."